Spontaneous creation of macroscopic flow and metachronal waves in an array of cilia

Boris Guirao, Jean-François Joanny

Spontaneous creation of macroscopic flow and metachronal waves in an array of cilia

Boris Guirao[1]
Laboratoire Physico-chimie Curie (UMR 168),
Institut Curie, Paris, France

Jean-François Joanny
Laboratoire Physico-chimie Curie (UMR 168),
Institut Curie, Paris, France

[1]Corresponding author. Address: Laboratoire Physico-chimie Curie (UMR 168), Institut Curie, 26 rue d'Ulm, 75248, Paris Cedex 05, France, Tel.: (+33)1-42-34-64-71, Email: boris.guirao@m4x.org

Abstract

Cells or bacteria carrying cilia on their surface show many striking features : alignment of cilia in an array, two-phase asymmetric beating for each cilium, coordination between cilia and existence of metachronal waves with a constant phase difference between two adjacent cilia. We give simple theoretical arguments based on hydrodynamic coupling and an internal mechanism of the cilium derived from the behavior of a collection of molecular motors, to account qualitatively for these cooperative features. Hydrodynamic interactions can lead to the alignment of an array of cilia. We study the effect of a transverse external flow and obtain a two-phase asymmetrical beating, faster along the flow and slower against the flow, proceeding around an average curved position. We show that an aligned array of cilia is able to spontaneously break the left-right symmetry and to create a global average flow. Metachronism arises as a local minimum of the beating threshold and leads to a rather constant flow.

Key words: cilia; coordination; beating; symmetry breaking; hydrodynamic interactions; metachronal waves

1 Introduction

Many cells and bacteria have cilia or flagella on their surfaces. Examples are sperm cells which have one flagellum used for propulsion, the green alga *Chlamydomonas* that uses two flagella, and the much studied protozoan *Paramecium* which is covered by a layer of cilia. This layer is made out of approximately four thousands cilia which produce a very efficient motion with a velocity of order $1mm/s$ in water, corresponding to 10 times the *Paramecium* size/s. Humans have ciliated cells in several organs: in the brain (cerebrospinal fluid flow), the retina (photoreceptor connective cilia), the respiratory tract (epithelial cells), the ear (hair bundles), the Falopian tube or the kidney...

Cilia have two major roles: (i) detection (sensory cilia or flagella), for example in the retina, the ear and the kidney (ii) propulsion or creation of fluid flow (motile cilia or flagella) as for *Paramecium* or in the respiratory tract where the fluid flow is used to move away the mucus.

The common structure of most cilia and flagella is an axoneme wrapped by the plasma membrane. The (9+2) axoneme is made of 9 microtubule doublets arranged on a circle around a central pair of microtubules (1). The cilium or flagellum is attached to the cell membrane by a basal body made of 9 microtubule triplets which has a structure very similar to that of a centriole. The basal body is attached to the cell membrane by anchoring fibers (2). Typically the radius of an axoneme is 100 nm. The main structural difference between cilia and flagella is their length. The typical length of a cilium is $10\mu m$ whereas a flagellum can be ten times longer.

Dynein molecular motors are attached to the 9 microtubule doublets; they move towards the microtubules $-$ ends linked to the basal body and exert forces on the microtubules. Upon consumption of Adenosine-Tri-Phosphate (ATP), dynein motion generates forces that induce a sliding between adjacent microtubules. Because the whole structure is attached at its basis, this sliding motion induces the bending of the cilium or flagellum and its beating.

We here focus on ciliated cells creating fluid flow. These are cells with cilia on their surface, beating in one preferred direction in a coordinated way. One central feature of cilia beating is the existence of two phases with a broken symmetry. Each beating can be decomposed into an effective stroke (ES) that propels the fluid and a recovery stroke (RS) where the cilium is coming back against the flow. In the example of *Paramecium* in water, the effective stroke lasts typically 9ms whereas the recovery stroke lasts 26ms.

The typical beating frequency in water is $30Hz$ (3). The beating of *Paramecium* cilia is 3-dimensional but for some species like *Opalina* the cilia remain in the same plane during their beating and the beating is 2-dimensional. In this work, we discuss the role of an external velocity field in this left-right symmetry breaking between the effective stroke and the recovery stroke for planar beating.

One of the most striking features of an assembly of beating cilia is that they all beat in the same direction: the surrounding fluid can only be propelled efficiently if all the beatings have the same orientation. In all mature ciliated cells, the beating direction is defined by the anchoring of the basal foot on the basal body. Only newly formed or developing cilia are randomly oriented (4). When they start beating, they tend to spontaneously align to finally beat in the same direction. One of the questions addressed in this article is the nature of the parameters that control this orientation.

The role of the central pair of microtubules in the center of the axoneme is also a fundamental and complex question. In many species (such as *Chlamydomonas*), the central pair is both rotating and twisting within the axoneme during the axoneme movement. Current models postulate that the central pair modulates dynein activity along outer microtubule doublets (5). It thus allows the axoneme motion because if all the dyneins were acting at the same time, no bending would occur. Evidence in support of this model includes the observation that sliding between adjacent doublets occurs preferentially along doublets closest to one of the two microtubules of the central pair (the C1) in *Chlamydomonas* flagella (6). Nevertheless, there exist also motile cilia with a (9+0) axoneme having no central pair. This means that cilia beating is possible even in the absence of the central pair of microtubules. Despite its importance, we do not discuss the role of the central pair in the present work and we postpone its discussion to future work.

Another important feature of ciliated cells, is the existence of waves propagating all along the surface. These are called metachronal waves and might be due to the coordination of adjacent cilia for example via hydrodynamic interactions. Experimentally metachronal waves are observed to propagate in all possible directions: in the direction of the effective stroke (symplectic metachronal waves), in the opposite direction (antiplectic), or even in a perpendicular (laeoplectic or dexioplectic) or oblique direction. The origin of these waves and the mechanisms controlling their formation are not well understood. We show in this article that metachronism can arise naturally from the hydrodynamic couplings between cilia. Using a two-state model

for the dynein motion as an internal mechanism of the cilia, metachronism appears to be a local minimum in the oscillation threshold of the motors (7, 8).

A last important feature of cilia beating that we wish to mention, is the role of calcium ions. The local $[Ca^{2+}]$ concentration has a strong influence on the beating pattern of cilia or flagella. For example detergent-treated *Paramecium* are able to swim forward at low $[Ca^{2+}]$ concentration ($< 10^{-6}M$) and backward at high $[Ca^{2+}]$ concentration ($> 10^{-6}M$) because of ciliary reversal: the directions of effective and recovery strokes are switched (9, 10). In any case, the wild type *Paramecium* can have a very efficient backward motion monitored by calcium tanks in its body. We only discuss here qualitative aspects of the role of calcium.

In this paper, we address the question of the spontaneous alignment of an array of beating cilia and the possibility of a spontaneous symmetry breaking in the beating that leads to the appearance of a macroscopic fluid flow. The internal mechanism of the cilia is described by the model of references (7, 8) which is based on a two-state model to describe the cooperative effects between dynein motors and only considers the relative sliding of two microtubules in the axoneme. The coordination between the cilia is due to hydrodynamic interactions which are discussed in details in a coarse-grained description where the effect of the cilia on the flow is replaced by an effective force. The outline of the paper is as follows. In the next section, we give a simple model for the alignment of beating cilia. In section 3, we discuss the beating of one cilium following the model of Jülicher and Camalet (7, 8). Finally, in section 4 we discuss the spontaneous breaking of the left-right symmetry of the beating due to the flow created by the cilia themselves.

2 Spontaneous alignment of an array of cilia: a simple model

2.1 Experimental results

In an assembly of cilia covering the surface of a mature cell, cilia are beating in a preferred direction, and only newly formed or developing cilia are randomly oriented (4). We first discuss the experiments showing how this preferred orientation is chosen.

As mentioned before, the ciliary axoneme grows from a basal body analogous to a centriole. Two basal body appendages, the basal foot and the striated rootlet, located in the axial plane of the effective stroke, confer an asymmetrical organization to the basal body. The basal foot is laterally associated with two consecutive triplets and points in the direction of the effective stroke (11, 12). The striated rootlet, associated with the proximal end of the basal body, sinks into the cytoplasm in the opposite direction (11). These two appendages define therefore an orientation of a cilium independent of the beating motion.

During ciliogenesis, newly formed basal bodies migrate toward the cell membrane where they anchor with no apparent order. Anchoring induces axoneme assembly, and cilia grow in random orientations. While cilia are growing, they do not beat immediately. A reorientation by rotation of the basal bodies in a common direction occurs at the final stage of ciliogenesis, when mature cilia beat (13). The preferred direction of the assembly is then well-defined. In the immotile-cilia syndrome, axonemes are incomplete, and the ciliary activity is abnormal or absent: the fluid is poorly or not propelled. On the cell level, the basal bodies are randomly oriented (14).

These experimental facts suggest that the beating and orientation of cilia are closely related. Our working hypothesis is that the alignment of an assembly of beating cilia is mostly due to hydrodynamical coupling between cilia. The global flow created by the other cilia tend to orient a given cilium and above a certain beating amplitude, all cilia orient in the same direction. We now give a very simple modelling of this cooperative alignment.

2.2 Alignment transition

We assume in the following that the beating is planar. It is the case for *Opalina* for example, but not exactly for *Paramecium* where the recovery stroke is not in the plane of the effective stroke.

Near the top of the ciliary layer, observations show that the velocity is time independent and uniform (15). Consequently, we average the beating over one time period and replace each cilium of length L (and its effective and recovery stroke) by a single force (stokeslet) $\vec{f}$, parallel to the surface, created in the fluid of viscosity η at height $h < L$ above the membrane, as sketched in figure 1.

We choose the x axis in the direction of the effective stroke and the z axis perpendicular to the cell surface that we approximate by a plane. The

stokeslet along the x axis ($\vec{f} = f\vec{e_x}$), is located at point $\vec{S} = (0, 0, h)$.

The velocity created at point $\vec{X} = (x, y, z)$ by this stokeslet with a no-slip boundary condition on the plane $z = 0$ is given by :

$$\vec{v}(\vec{X}) = \mathbf{G}(\vec{X}, \vec{S}).\vec{f}$$

where the response tensor tensor $\mathbf{G}$ is given in (16) and reads:

$$\begin{aligned} 8\pi\eta\ \mathbf{G}_{jk}(\vec{X}, \vec{S}) = &\left(\frac{\delta_{jk}}{\rho} + \frac{\rho_j\rho_k}{\rho^3}\right) - \left(\frac{\delta_{jk}}{R} + \frac{R_jR_k}{R^3}\right) \\ &+2S_z\left(\delta_{k\alpha}\delta_{\alpha l} - \delta_{kz}\delta_{zl}\right)\frac{\partial}{\partial R_l}\left(\frac{S_zR_j}{R^3} - \frac{\delta_{jz}}{R} - \frac{R_jR_z}{R^3}\right) \end{aligned} \tag{1}$$

where $\vec{\rho} = \vec{X} - \vec{S}$, $\vec{R} = \vec{X} + \vec{S}$ and $\alpha = x, y$.

In order to simplify the hydrodynamic problem, we assume in all the following that the cilia are far away from each other. In this asymptotic limit, it is consistent to describe the effect of the cilium in the fluid by a stokeslet. We introduce the two-dimensional vector along the cell surface $\vec{r} = (x, y)$ and consider the limit $r \gg z, h, L$. We are interested in the velocity in the vicinity of the ciliary layer, typically $0 < z < 1.5\ L$. At lowest order in z/r, the velocity reads:

$$\vec{v}(r, \theta, z) = \frac{3fh}{2\pi\eta}\frac{z\cos\theta}{r^3}\vec{e_r} + \mathcal{O}(z^3/r^3) \simeq \vec{u}(r, \theta)\ \bar{z} \tag{2}$$

where we have defined a dimensionless height $\bar{z} = z/L$. In the following, we use mostly the velocity $\vec{u}(r, \theta)$. At this order, the flow field is a radial flow centered on the cilium-stokeslet. Note that because of the no slip boundary condition on the surface, the force appears in the velocity field (Eq. 2) in the combination fh homogeneous to a momentum.

We consider now a regular array of cilia; this is a reasonable assumption for *Paramecium*, which shows a beautiful and very regular array of cilia on its surface (17). We assume that this array is in an infinite plane. Cilium i is defined by its position in the x, y plane (the cell surface) by a vector $\vec{r_i}$ and by the angle of its plane of beating with the x axis, ϕ_i as displayed on Fig. 2.

The total velocity at the cilium i at height z, $\vec{V}(\vec{r_i}, z)$ is the sum of all

the velocities $\vec{v}_j(\vec{r}_i, z)$ created by the other cilia $j \neq i$:

$$\vec{V}(\vec{r}_i, z) = \sum_{j \neq i} \vec{v}_j(\vec{r}_i, z)$$

We single out the the $\bar{z}$ dependence of $\vec{V}$ writing $\vec{V}(\vec{r}_i, z) = \vec{U}(\vec{r}_i)\ \bar{z}$ with $\vec{U}(\vec{r}_i) = \sum_{j \neq i} \vec{u}_j(\vec{r}_i)$ and

$$\vec{u_j}(\vec{r_i}) \simeq \frac{3fhL}{2\pi\eta} \frac{\cos(\theta_{ji} - \phi_j)}{|\vec{r_i} - \vec{r_j}|^3} \vec{e_{ji}} \tag{3}$$

where $\vec{e_{ji}}$ is a unit vector from cilium j to cilium i and $\theta_{ji} = (\vec{e_x}, \vec{e_{ji}})$, as shown on Fig. 2.

We now use a mean field approximation, replacing the velocity $\vec{u}_j(\vec{r}_i)$ by its average over the directions $< \vec{u}_j(\vec{r}_i) >_\phi$ given by:

$$< \vec{u_j}(\vec{r_i}) >_\phi = \int_0^{2\pi} d\phi\ P(\phi)\ \vec{u_j}(\vec{r_i}) \tag{4}$$

where $P(\phi)$ is the probability for a cilium to make an angle ϕ with the x axis. The average velocity at cilium i is $\vec{U}(\vec{r}_i) \simeq \sum_{j \neq i} < \vec{u}_j(\vec{r}_i) >_\phi$.

The mean field approximation assumes that the fluctuations around a given angle determining the direction of the flow are small. We choose the x axis in the direction of the flow without any loss of generality, so that the probability $P(\phi)$ is peaked around $\phi = 0$.

In order to determine the probability $P(\phi)$, we write a stationary Fokker-Planck equation $\partial_\phi J = 0$. The probability current $J = P\partial_t\phi - D_r\partial_\phi P$ is the sum of two terms: a convection term and a diffusion term where D_r is a rotational diffusion coefficient. The beating plane can fluctuate due to thermal fluctuations. Because of the flow, if the beating plane of one cilium is at an angle ϕ with the flow direction, the cilium is subject to a torque $M_z^{flow} = -\alpha U \sin\phi$ along the z axis that tends to align it in the direction of the flow, where $U\bar{z}$ is the velocity of the global flow and α a viscous coefficient involving the geometry of the cilium. A rotating cilium is also subject to a viscous torque $M^{viscous}$ opposing the rotation $M_z^{viscous} = -\zeta\partial_t\phi$ where ζ is the rotational friction constant. The total torque on the cilium vanishes ($M_z^{flow} + M_z^{viscous} = 0$) and the probability distribution satisfies the

Fokker-Planck equation

$$\frac{\partial^2 P}{\partial \phi^2} + \frac{\alpha U}{D_r \zeta} \frac{\partial}{\partial \phi}[P \sin \phi] = 0$$

Defining the effective temperature as $D_r \zeta = k_B T$ and imposing the normalization condition $\int P(\phi) d\phi = 1$, we obtain:

$$P(\phi) = \frac{e^{\frac{\alpha U}{k_B T} \cos \phi}}{2\pi I_0(\frac{\alpha U}{k_B T})} \tag{5}$$

where $I_0(x)$ is the modified Bessel function defined in (18). The average velocity $\vec{U}$ can then be self-consistently determined by calculating $< \vec{u}_j(\vec{r}_i) >_\phi$, and summing over all the lattice sites. We obtain

$$\vec{U} = \frac{3fhL}{2\pi\eta d^3} \; K \; \frac{I_1(\frac{\alpha U}{k_B T})}{I_0(\frac{\alpha U}{k_B T})} \; \vec{e_x} \tag{6}$$

where K is a constant depending on the nature of the lattice, d is the lattice constant (the distance between cilia) and I_1 is a modified Bessel function (18). For a square lattice, (19):

$$K_{square} = \sum_{(k,l) \neq (0,0)} \frac{k^2}{(k^2 + l^2)^{5/2}} = 2 \; \beta(\frac{3}{2}) \zeta(\frac{3}{2}) \simeq 4.52 \tag{7}$$

$\beta(s)$ and $\zeta(s)$ being respectively the Dirichlet and the Riemann functions (18).

The self-consistent equation for the flow velocity can be discussed by expanding the integrals I_0 and I_1 in the vicinity of $U = 0$: there are two solutions $U = 0$, and a solution at a finite velocity which exists only within a certain range of parameters

$$U = 2\sqrt{2} \frac{k_B T}{\alpha} \; \sqrt{1 - \frac{4\pi k_B T \eta d^3}{3K\alpha f h L}} \tag{8}$$

This solution exists only if

$$\frac{3K\alpha f h L}{4\pi k_B T \eta d^3} > 1 \tag{9}$$

Within the mean field approximation Eq. 9 defines a dynamical phase transition between a non-moving fluid with randomly oriented cilia and a moving fluid with a global flow $V(z) = U\bar{z} \neq 0$ given by Eq. 8 where all cilia are spontaneously aligned in the same orientation. This dynamical phase transition is second order (with a continuous velocity at the transition) and it is associated to a spontaneous breaking of the initial $O(2)$ symmetry.

The influence of some of the parameters can be directly analyzed on Eq. 9. A decrease of the distance d between two cilia favors the alignment, increasing the hydrodynamic coupling. A decrease of the temperature T also favors alignment as the random thermal motion opposes the alignment. An increase of the effective hydrodynamic force of one cilium f is associated to an increase the hydrodynamic interactions between cilia and leads to a better alignment. The same effect occurs for α and the cilium length L. Finally, increasing h helps to create a global flow, since the velocity on the membrane vanishes and the higher the force is exerted, the more efficient.

A more precise analysis requires the estimation of the parameters f, α and h. The height is of the order of the cilium size $h \sim L$. The calculation of α is given in appendix I for a general beating (Eq. 54). It turns out that α is linked to the difference of the areas covered during the effective and recovery strokes. Here we approximate $\alpha \sim \xi_\perp L\mathcal{A}$, where $\xi_\perp$ is the perpendicular friction constant per unit length of the cilium and $\mathcal{A}$ the amplitude of the movement of the tip.

In order to give a simple estimation of the effective hydrodynamic force, we consider that the friction coefficient takes the perpendicular value $\xi_\perp$ during the effective stroke, and the parallel value $\xi_\parallel$ during the recovery stroke. Introducing the beating frequency ω, we estimate $f \sim (\xi_\perp - \xi_\parallel) L\omega\mathcal{A}$. A more precise calculation of these two quantities as a function of the beating patterns is given in appendix I.

Consequently, we obtain:

$$\frac{3K\alpha f h L}{4\pi k_B T \eta d^3} \sim \frac{\xi_\perp(\xi_\perp - \xi_\parallel)\mathcal{A}^2 L\omega}{k_B T \eta} \frac{L^3}{d^3}$$

The difference between the two local drag coefficients $\xi_\perp$ and $\xi_\parallel$ is the key to

an efficient beating. Increasing the amplitude $\mathcal{A}$ or the frequency ω of the beating favors the alignment of cilia, as could be expected. Increasing the viscosity of the medium also promotes the transition, because it increases the coupling between cilia.

This naive mean field approximation is only a first step of our study. In the following, we take a closer look at the internal beating mechanism of one cilium and then at the beating of an array of cilia to obtain a more precise and quantitative description.

3 Axonemal beating

In this section we discuss the beating mechanism of a single cilium. We follow closely the work of Camalet and Jülicher (8) which mimics the cilium by two microtubule filaments sliding along one another under the action of the dynein motors and uses a 2-state model to describe the collective motion of the dyneins. We use as boundary conditions for the motion those introduced recently by Hilfinger and Jülicher (20) that seem to have good experimental support (21). In the next section, we use the same model to discuss the coordination between cilia.

3.1 Equation of motion

Each microtubule doublet within the axoneme can be described effectively as an elastic rod. Deformations of this rod lead to local sliding displacements of neighboring microtubules. Here, we only consider planar deformations. In this case the geometrical coupling between bending and sliding can be captured by considering two parallel elastic filaments (corresponding to two microtubule doublets) with a constant separation a along the whole length of the rod (see Fig. 3). At one end, which corresponds to the basal end of an axoneme, the two filaments are elastically attached and are allowed to slide with respect to each other, but not to tilt (20). The basal connection is characterized by an elasticity k and a frictional drag γ. The configurations of the axoneme are described by the shape of the filament pair given by the position of one filament $\vec{X}(s)$ at arclength s. The shape of the other filament is then given by $\vec{X}'(s) = \vec{X}(s) - a\vec{n}(s)$, where $\vec{n}$ is the filament normal. In the following, we describe the filament conformation by the angle ψ between the local tangent vector and the z axis or by the deformation h in the transverse

direction defined in Fig. 11.

The energetics of the filament pair is due to the bending elasticity. In addition to filament bending, we also take into account internal stresses due to the active elements (dyneins). We characterize them by the force per unit length $f(s)$ acting at position s in opposite directions on the two microtubules. This force density corresponds to a shear stress within the cilium which tends to slide the two filaments with respect to each other.

The local curvature is $C = \partial_s \psi$ (see Fig. 11). The sliding displacement, $\Delta(s,t)$ is related to the the sliding displacement at the base $\Delta_0(t)$ by $\Delta(s,t) - \Delta_0(t) = a\psi(s,t)$, because we impose the boundary condition $\psi(0,t) = 0$.

A configuration of a filament pair of length L is associated to the free energy functional:

$$G = \frac{k}{2}\Delta_0^2 + \int_0^L ds[\frac{\kappa}{2}C^2 - f\Delta + \frac{\Lambda}{2}(\partial_s \vec{X})^2]$$

Here, κ denotes the total bending rigidity of the filaments. The inextensibility of the filaments is taken into account by the Lagrange multiplier $\Lambda(s)$ which enforces the constraint $(\partial_s \vec{X})^2 = 1$.

The first term of this equation is the elastic energy due to the basal sliding occurring with a connection of elasticity k.

The tangent component of the integrated forces acting on the filament between s and L is denoted by $\tau(s)$. Assuming that there is no external force applied at the end $s = L$ of the cilium:

$$\tau(s) = \vec{t}(s).\int_s^L ds' \ \frac{\delta G}{\delta \vec{X}} = -\vec{t}(s).\int_0^s ds' \ \frac{\delta G}{\delta \vec{X}}$$

We assume for simplicity, that the hydrodynamic effects of the surrounding fluid can be described by two local friction coefficients $\xi_\perp$ and $\xi_\parallel$ for normal and tangential motion. The total friction force per unit length exerted by the cilium on the fluid is then $\vec{f}_v[\vec{X}(s)] = (\xi_\parallel \vec{t}\,\vec{t} + \xi_\perp \vec{n}\,\vec{n})\ \partial_t \vec{X}(s)$. The force balance at arclength s can then be written as

$$\partial_t \vec{X} = -(\frac{1}{\xi_\perp}\vec{n}\,\vec{n} + \frac{1}{\xi_\parallel}\vec{t}\,\vec{t})\ \frac{\delta G}{\delta \vec{X}} \tag{10}$$

which leads to:

$$\partial_t \vec{X} = \frac{\vec{n}}{\xi_\perp}(-\kappa\dddot{\psi} - a\dot{f} + \dot{\psi}\tau) + \frac{\vec{t}}{\xi_\parallel}(\kappa\dot{\psi}\ddot{\psi} + a\dot{\psi}f + \dot{\tau}) \tag{11}$$

where the derivatives with respect to arclength have been denoted by a dot.

The beating of the filaments is very sensitive to the boundary conditions imposed at its ends. As the the force density $-\delta G/\delta\vec{X}$ is equilibrated by the density of friction force exerted by the fluid on the system (see Eq. 10), the boundary contributions coming from the free energy variation δG are equilibrated by external forces $\vec{f}_{ext}$ and torques $\vec{T}_{ext} = T_{ext}\ \vec{e}_y$ applied at the ends.

At the free end of the cilium, both the external force and the external torque vanish and

$$\vec{f}_{ext} = -\left(\kappa\dot{C} + af\right)\vec{n} + T\vec{t} = \vec{0}, \quad T_{ext} = \kappa C = 0 \tag{12}$$

At the base, $s = 0$, the boundary conditions are:

$$\vec{f}_{ext} = \left(\kappa\dot{C} + af\right)\vec{n} - T\vec{t}, \quad T_{ext} = -\kappa C + a\int_0^L ds f(s) \tag{13}$$

The external torque and force are chosen in such a way that the base is fixed ($\partial_t\vec{X} = \vec{0}$) and that the cilium remains perpendicular to the surface ($\partial_t\vec{t} = \vec{0}$ or $\psi(0) = 0$).

The final boundary condition is associated to the basal sliding

$$\gamma\partial_t\Delta_0 = -\frac{\delta G}{\delta\Delta_0} = -k\Delta_0 + \int_0^L ds f(s) \tag{14}$$

The determination of the cilium motion requires a model for the shear force created by the dyneins that we calculate using a two-state model.

3.2 2-state model for the cilium

Following (8), we now introduce the 2-states model of coupled molecular motors (22, 23) to describe the internal mechanism of the cilium. This model allows the calculation of the shear force f due to the dyneins.

Each motor has two different chemical states, a strongly bound state,

1, and a weakly bound state, 2. The interactions between a motor and a filament in both states are characterized by potential energy landscapes $W_1(x)$ and $W_2(x)$, where x denotes the position of a motor along the filament. The potentials have the filament symmetry: they are periodic with period l, $W_i(x) = W_i(x+l)$ and are, in general, spatially asymmetric, $W_i(x) \neq W_i(-x)$.

In the presence of ATP, the motors undergo transitions between states with transition rates ω_1 and ω_2. Introducing the relative position ξ of a motor with respect to the potential period, ($x = \xi + nl$ with $0 \leq \xi < l$ and n an integer), we define the probability $P_i(\xi, t)$ for a motor to be in state i at position ξ at time t. The relevant Fokker-Planck equations are:

$$\begin{aligned} \partial_t P_1 + v\ \partial_\xi P_1 &= -\omega_1 P_1 + \omega_2 P_2 \\ \partial_t P_2 + v\ \partial_\xi P_2 &= \omega_1 P_1 - \omega_2 P_2 \end{aligned}$$

where $v = \partial_t \Delta = a \partial_t \psi(s)$ is the sliding velocity between the 2 filaments.

The simplest choice of the two potentials W_i, is a saw-tooth potential (with barrier height $U \gg kT$) representing a strongly bound state for W_1, and a flat potential W_2 representing a weakly bound state. Here, for simplicity, we use the symmetric potentials:

$$\begin{aligned} W_1(x) &= U \sin^2(\pi \frac{x}{l}) \\ W_2(x) &= W_2 \end{aligned}$$

Although this choice is somehow arbitrary, we checked that the final results only depend qualitatively on the actual shape of the potentials and of the rates defined below.

When a number of motors act together to propel a filament, however, the direction of motion is a collective property. The filament might move in either direction (23). The absence of asymmetry in the potentials implies that an individual motor is not able to move directionally. It is not the case for an assembly of motors: even with a symmetric potential, provided that detachment can only take place at a localized position near the bottom of a potential well, oscillations can occur.

We define the distance from equilibrium Ω:

$$\Omega = Sup_{[0,l[} \mid \frac{\omega_1}{\omega_2} - e^{\frac{W_1 - W_2}{kT}} \mid \propto e^{\Delta\mu/kT} - 1 \qquad (15)$$

Ω is related to the chemical potential difference between ATP and its hydrolysis products, $\Delta\mu = \mu_{ATP} - \mu_{ADP} - \mu_P$. At equilibrium, $\Delta\mu = 0$ and $\Omega = 0$. We assume for simplicity that the binding rates ω_2 and the detachment rate ω_1 are given by:

$$\begin{aligned} \omega_2(\xi) &= \nu(1 + \Omega \sin^2(\pi \frac{\xi}{l})) \\ \omega_1(\xi) &= \nu\Omega \cos^2(\pi \frac{\xi}{l}) \end{aligned}$$

Note that, with this choice the sum $\omega_1 + \omega_2 = \nu(1 + \Omega)$ does not depend on ξ, and that if $\Omega = 0$, $\omega_1 = 0$ and no directional movement is possible. Here ν is a constant transition rate.

If we assume that the motors are uniformly distributed along the filaments with a density ρ, the probabilities P_1 and P_2 satisfy the relationship $P_1 + P_2 = \rho$. The Fokker Planck equation reduces then to a single equation for $P = P_1$

$$\partial_t P + (\partial_t \Delta)\partial_\xi P = -(\omega_1 + \omega_2)P + \rho\omega_2(\xi) \tag{16}$$

This model leads to an expression for the shear force per unit of length $f(s,t)$ created by the dyneins and driving the the cilium beating. Using the results of (22), and the fact that W_2 is a constant:

$$f(s,t) = -K\Delta - \lambda\partial_t\Delta - \frac{1}{l}\int_0^l d\xi \; P(\xi)\partial_\xi W_1 \tag{17}$$

where K is an elastic stiffness per unit length mimicking the influence of the nexins which are proteins acting as springs in the axonemal structure, and λ is an internal friction coefficient per unit length modelling the friction encountered by the motors. Equations 11 and 16 allow in principle a complete calculation of the beating motion.

In the following, we assume that the beating occurs with a "small" amplitude which means that both $\psi(s,t) \ll 1$ and $h(s,t) \ll L$. A quick look at the beating pattern of a cilium of *Paramecium* shows that the beating occurs with a large amplitude. Nevertheless, this approximation allows us to extract interesting information on the parameters controlling the beating. Moreover, the work of Hilfinger shows that larger amplitude beating patterns are very similar to small amplitude patterns (20). We must however keep in mind that our approach is valid only if the the system stays close to an

oscillation bifurcation which is consistent with the fact that we consider only small movements.

We use the deformation h, rather than ψ or Δ to describe cilium motion and work at second order in $|h|$ so that $\psi = \dot{h} + \mathcal{O}(|h|^3)$. In the absence of any external flow, the equation of motion 11 projected on $\vec{t}$ imposes that $\tau = \mathcal{O}(|h|^2)$. The projection of the equation of motion on $\vec{n}$ then yields:

$$\xi_\perp \partial_t h = -\kappa \ddddot{h} - a\dot{f} + \mathcal{O}(|h|^3) \tag{18}$$

The non-linear terms are not important here but they will turn out important in the following section. Indeed, experiments show that the beating is clearly asymmetrical (ES and RS), and we must expand at least to next order if we want to capture this phenomenon. With this variable and at this order, the boundary conditions read:

$$\begin{aligned} h(s=0) = 0, \quad \dot{h}(s=0) = 0 \\ \kappa \dddot{h}(s=L) + af(s=L) = 0, \quad \ddot{h}(s=L) = 0 \end{aligned} \tag{19}$$

The explicit solution of the equation of motion 18 is obtained by Fourier expansion in time $h(s,t) = \sum_{n=-\infty}^{\infty} h_n(s) e^{in\omega t}$. The explicit derivation of the equation satisfied by the Fourier components is given in appendix II. At linear order the effect of the motors is characterized by a susceptibility

$$\chi(\Omega, \omega) = -K - \lambda i\omega + \frac{\pi^2 \rho U}{2l^2} \frac{i\Omega\omega}{(1+\Omega)((1+\Omega)\nu + i\omega)} \tag{20}$$

Using dimensionless variables, $\bar{s} = s/L$, $\bar{\omega} = \dfrac{\xi_\perp L^4}{\kappa}\omega$, $\bar{\chi}_n = \dfrac{a^2 L^2}{\kappa}\chi(\Omega, n\omega)$ and $\bar{h} = h/L$, the equation of motion for the Fourier component n reads

$$\ddddot{\bar{h}}_n + \bar{\chi}_n \ddot{\bar{h}}_n + in\bar{\omega}\, \bar{h}_n = 0 \tag{21}$$

The boundary conditions at the base $\bar{s} = 0$ are

$$\bar{h}_n(0) = 0, \quad \dot{\bar{h}}_n(0) = 0 \tag{22}$$

At the free end of the cilium, $\bar{s} = 1$:

$$\dddot{\bar{h}}_n(1) + \bar{\chi}_n \dot{\bar{h}}_n(1) + \bar{\Gamma}_n \bar{h}_n(1) = 0, \quad \ddot{\bar{h}}_n(1) = 0 \tag{23}$$

with $\bar{\Gamma}_n = \bar{\chi}_n^2 / \left(\bar{k} - \bar{\chi}_n + in\bar{\gamma}\bar{\omega}\right)$ where we have introduced the dimensionless parameters $\bar{k} = \dfrac{a^2 L}{\kappa} k$ and $\bar{\gamma} = \dfrac{a^2}{L^3 \xi_\perp} \gamma$.

3.3 Beating pattern

In the absence of any external flow the beating is symmetric and the Fourier components n=0 and n=2 of h vanish for symmetry reasons. Close to the oscillation bifurcation threshold, cilium beating is dominated by the first Fourier component $n = 1$.

The solution of the linear equation of motion 21 is written as the sum of 4 exponentials

$$\bar{h}_1(\bar{s}) = \mathcal{A}_1 \left(e^{q_1 \bar{s}} + b_1 e^{-q_1 \bar{s}} + c_1 e^{q_2 \bar{s}} + d_1 e^{-q_2 \bar{s}} \right) \tag{24}$$

where the two inverse decay lengths are given by

$$q_1 = \left(-\frac{\bar{\chi}_1}{2} + \frac{1}{2} (\bar{\chi}_1^2 - 4i\bar{\omega})^{1/2} \right)^{1/2}, \quad q_2 = \left(-\frac{\bar{\chi}_1}{2} - \frac{1}{2} (\bar{\chi}_1^2 - 4i\bar{\omega})^{1/2} \right)^{1/2} \tag{25}$$

The boundary conditions are explicitly discussed in appendix II. The condition for existence of non vanishing solutions is given by equation 63 of Appendix II. This is a complex equation, that gives therefore two conditions which determine both the the critical value of the distance from equilibrium where the oscillations start Ω_c, and the reduced oscillation frequency $\bar{\omega}_c$. The critical value Ω_c is a Hopf bifurcation threshold: there are no oscillations if $\Omega \leq \Omega_c$ and cilium beating is only possible if $\Omega \geq \Omega_c$. At the bifurcation threshold, the amplitude of the oscillations vanishes. It is not possible to calculate the amplitude of the oscillations above the bifurcation threshold with the linear theory presented here. This requires a complete determination of the third order terms in the equation of motion which goes far beyond the scope of this work. This very complex problem is attacked in the work of Hilfinger and Jülicher (20).

An analytical determination of the Hopf bifurcation threshold and of the beating frequency at the threshold does not seem to be possible analytically. We therefore rely on a numerical solution, choosing reasonable values of the various parameters.

We study a cilium of length $L = 12\mu m$, which is the length of a *Parame-*

cium cilium. It moves in a fluid of viscosity $\eta \sim 4\eta_{water} = 4\ 10^{-3} Pa.s$, which is higher than the water viscosity in order to take into account the proteins above the cell body. We estimate $\kappa = 4\ 10^{-22} J.m$ corresponding to 20 microtubules (24). The other parameters are $l = 10nm$, $a = 20nm$, $U = 10kT$, $K \simeq 0$, $\rho = 5\ 10^{8} m^{-1}$, and $\lambda = 1 Pa.s$ very similar to those of (7). In order to match the typical frequency observed in *Paramecium*, and to obtain a realistic pattern of the beating, we take $\xi_\perp = 35.5\eta = 142\ 10^{-3} Pa.s$ and we choose $k = 6.54 Nm^2$, $\gamma = 7.31\ \eta_{water}$, and $\nu = 600 s^{-1}$.

The value of $\xi_\perp$ is rather high, but it must include the hydrodynamic interactions of the cilium with the cell surface (see (25)) which are not taken into account if we use the classical friction per unit length of a rod.

The numerical resolution of Eq. 63 then yields $(\Omega_c, \bar{\omega}_c) \simeq (6.55\ 10^{-9}, 1294)$. This corresponds to a critical beating frequency $f_c \simeq 28 Hz$ which is the typical value for *Paramecium* (3). The calculated beating pattern of the cilium is shown on figure 4. It corresponds to a wave (or a superposition of waves) propagating from the base of the cilium to the free tip as observed experimentally.

A detailed study shows that the equation giving the bifurcation threshold and the beating frequency has several solutions. $(\Omega_c^{(n)}, \bar{\omega}_c^{(n)})$ with $\Omega_c^{(n+1)} > \Omega_c^{(n)}$. A first guess would be that the axoneme starts beating at the lowest threshold $(\Omega_c^{(1)}, \bar{\omega}_c^{(1)})$. However, it is known experimentally that during the beating the deformation waves propagate from the base to the tip and not from the tip to the base (26). The first two oscillating modes correspond to waves propagating in the opposite direction. In order to be consistent with the experiments we do not consider them here. A better choice of the transition rates ω_1 and ω_2, would perhaps allow to justify this choice. The direction of propagation of the wave is extremely sensitive to the boundary conditions. We have allowed here basal sliding as suggested by some experiments and we have imposed that the cilium is clamped at its base with an angle $\psi = 0$. This also seems consistent with some experiments analyzed in (20). The other extreme limit of a completely free cilium (a vanishing external torque at the base) leads to a wave propagating form the base to the tip for the first mode. We have tried to use an intermediate boundary condition where the torque at the base is an elastic torque and varying the related stiffness, however we were not able to obtain a beating pattern looking like the experimental one. We therefore proceed, considering only the third beating mode.

The beating frequency f_c varies with the viscosity of the medium. Experimentally, when methyl-cellulose is added in water, the viscosity increases significantly. We predict here a decrease of f_c with increasing external viscosity as observed in the experiments of (27) and in numerical simulations (28) (see Table 1). We observe an approximate linear decrease of the beating frequency when plotted against $log(\eta/\eta_w)$ as in the simulations performed in (28) (we find similar values for the frequency).

The effect of $[Ca^{2+}]$ on the beating pattern can also be studied qualitatively. As mentioned in the introduction, $[Ca^{2+}]$ has a strong influence on the beating pattern. Calcium concentration variations are at the basis of the shock responses of many organisms, changing the ciliary-type beating into a flagellar-type beating in *Chlamydomonas*, or switching the directions of effective stroke and recovery stroke in *Paramecium*, or in reversing the direction of the "wave" propagation on the flagellum and thus reversing the direction of the movement in *Chritidia* (29).

This last example can be explained qualitatively within our approach. In *Chritidia*, both directions are possible for the deformation wave propagation. Calcium may affect the chosen mode of beating, allowing the system to choose $\Omega_c^{(1)}$ and its tip-to-base pattern instead of $\Omega_c^{(3)}$.

On the other hand, calcium is also likely to change the attachment/ detachment rate (and thus change the parameter ν) or the boundary conditions at the base of the cilium (and thus change k). In Chlamydomonas, calcium has a contractile effect on the striated fibers connecting the basal bodies of the two flagella (30). These changes induce a change in the beating pattern, and may result in a switch from base-to-tip to tip-to-base wavelike propagation.

4 Left-right beating symmetry breaking

In the presence of a transverse external flow, the beating can no longer be symmetrical as sketched on Fig. 5. The cilium tends to beat faster and quite straight in the direction of the flow, whereas it comes back slower and more curved against the flow. This looks like a two-phases beating with an effective and a recovery stroke.

If the beating is asymmetrical, the cilium exerts a force in the fluid that can itself produce a flow. In a certain range of parameters, one can therefore expect that a continuous flow is spontaneously generated by hydrodynamic

interactions between cilia: an assembly of cilia, beating symmetrically, is able to break spontaneously this left-right symmetry of the beating to create a global flow. This idea of a spontaneous breaking spontaneously of the left-right symmetry has already been suggested in (31) with a more abstract system (called rowers) having two internal energy states.

In this section, we first study the effect of an external velocity imposed by the experimentalist on the beating symmetry of a single cilium. We then consider an array of aligned cilia and determine the conditions under which this assembly of cilia breaks its left-right symmetry and generates a global flow. Metachronal coordination between cilia naturally emerges from hydrodynamic couplings as a local minimum of the oscillation threshold Ω_c.

4.1 External breaking of the beating symmetry: cilium submitted to an external flow

We impose an external flow $\vec{V} = V\vec{e_x}$ along the x axis for simplicity. It is found experimentally that the velocity above the cilia sub-layer is time independent and uniform (15), justifying our choice. This flow is in this first part externally fixed and we consider the limit of vanishingly small flows.

The force per unit length exerted by the cilium on the fluid $\vec{f_v}[\vec{X}(s)]$ depends on the external velocity $\vec{V}$.

$$\vec{f_v}[\vec{X}(s)] = (\xi_\parallel \vec{t}\,\vec{t} + \xi_\perp \vec{n}\,\vec{n})\ (\partial_t \vec{X}(s) - \vec{V}) \tag{26}$$

The equation of motion 11 reads then:

$$\partial_t \vec{X} = \vec{V} + \frac{\vec{n}}{\xi_\perp}(-\kappa\dddot{\psi} - a\dot{f} + \dot{\psi}\tau) + \frac{\vec{t}}{\xi_\parallel}(\kappa\dot{\psi}\ddot{\psi} + a\dot{\psi}f + \dot{\tau}) \tag{27}$$

The boundary conditions are the same as in the absence of the neighboring cilia and are given by Eq. 12, 13, 14.

Following the same procedure as for a cilium in the absence of flow, we find the equation of motion for the deformation of the cilium h:

$$\xi_\perp \partial_t h = \xi_\perp V - \kappa\ddddot{h} - a\dot{f} - \xi_\parallel V(h\ddot{h} + \frac{\xi_\perp}{2\xi_\parallel}\dot{h}^2) + \mathcal{O}(|h|^3) \tag{28}$$

The introduction of the external flow breaks the $h \longrightarrow -h$ symmetry (or

left-right symmetry) introducing in 18 terms of zeroth and second order in h in the equation of motion. The boundary conditions do not depend on the external flow.

As above, we expand the deformation of the cilium h in Fourier components in time. Using the same notations as before, the equation of motion of the Fourier components can be written as

$$\ddot{\bar{h}}_n + \bar{\chi}_n \ddot{\bar{h}}_n + in\bar{\omega}\, \bar{h}_n = \bar{V}\delta_{0,n} - \frac{\bar{V}}{2}(\bar{\xi}\, \bar{h}\ddot{\bar{h}} + \dot{\bar{h}}^2)_n \tag{29}$$

for $n = 0, 1, 2$ and where we have introduced the new dimensionless parameters:

$$\bar{V} = \frac{\xi_\perp L^3}{\kappa} V \qquad \bar{\xi} = \frac{2\xi_\parallel}{\xi_\perp}$$

In the limit of small external velocities, we have neglected terms of order $\bar{V}^2$.

The equation for the first mode is identical to Eq. 61, with the same boundary conditions. At this order in $\bar{V}$, the fundamental mode is not affected by the external flow. Consequently, the oscillation threshold and the beating frequency are the same as in the absence of flow and the Fourier component h_1 is given by Eq. 24.

The zeroth Fourier component $\bar{h}_0$ gives the average deformation of the cilium. It is a solution of

$$\ddot{\bar{h}}_0 - \bar{K}\, \ddot{\bar{h}}_0 = \bar{V} - \frac{\bar{V}}{2}\left[\bar{\xi}\, (\bar{h}_1 \ddot{\bar{h}}_1^* + \bar{h}_1^* \ddot{\bar{h}}_1) + |\dot{\bar{h}}_1|^2\right] \tag{30}$$

with the same boundary condition as before. Nevertheless, $\bar{h}_0$ does not vanish at first order in velocity because of the broken symmetry due to the external flow which is reflected in the right hand side of Eq. 30. The complete solution for $\bar{h}_0$ is rather tedious to obtain and lengthy. We do not display it here explicitly. We write it as the sum of two contributions; $\bar{h}_0^{Eq}$, corresponds to the curvature of the cilium under the flow V at equilibrium, i.e. in the absence beating ($\bar{h}_1 = 0$), and $\bar{h}_0^{ATP}$, corresponds to the corrections to this equilibrium deformation due to the beating when there is enough ATP in the medium $\bar{h}_0 = \bar{h}_0^{Eq} + \bar{h}_0^{ATP}$. If as above, we ignore the elasticity of the nexins

$(\bar{K} \to 0)$:

$$\begin{aligned} \bar{h}_0^{Eq}(\bar{s}) &= \frac{\bar{V}}{24}\bar{s}^2(\bar{s}^2 - 4\bar{s} + 6) \\ \bar{h}_0^{ATP}(\bar{s}) &= \frac{\bar{V}}{2}\mathcal{A}_1^2\phi_0(\bar{s}) \end{aligned} \tag{31}$$

where $\mathcal{A}_1$ is the amplitude of the first Fourier mode of the oscillation defined in Eq. 24 and $\phi_0(\bar{s})$ is a linear combination of exponentials. In the limit $V = 0$, $\bar{h}_0 = 0$ as expected. The average deformation of the cilium is plotted on Fig. 6 which shows the bent shape under the action of the external flow.

The second Fourier component gives the asymmetry of the beating. It is obtained from the equation of motion

$$\ddddot{\bar{h}}_2 + \bar{\chi}_2\,\ddot{\bar{h}}_2 + 2i\bar{\omega}\,\bar{h}_2 = -\frac{\bar{V}}{2}\left[\bar{\xi}\,\bar{h}_1\dddot{\bar{h}}_1 + \ddot{\bar{h}}_1^{\,2}\right] \tag{32}$$

We do not give here the lengthy explicit expression of $\bar{h}_2$ but we write it as

$$\bar{h}_2(\bar{s}) = \frac{\bar{V}}{2}\mathcal{A}_1^2\phi_2(\bar{s})$$

where $\phi_2(\bar{s})$ is a linear combination of exponentials. Here also, in the limit $V = 0$, $\bar{h}_2 = 0$. The plot $\bar{h}_2$ against $\bar{s}$ at different times on Fig. 6, leads to a complicated pattern.

The total deformation of the cilium $\bar{h}(\bar{s},t) \simeq \bar{h}_0(\bar{s}) + \bar{h}_1(\bar{s})e^{i\omega_c t} + \bar{h}_2(\bar{s})e^{2i\omega_c t} +$ *c.c.* is plotted against $\bar{s}$ at different times equally spaced on Fig. 7. In order to stress the fact that the beating is easier and faster in the direction of the flow, and more difficult and slower against the flow, we have chosen rather large values of the parameters, $\bar{\xi} = 1$, $\mathcal{A}_1 = 1/5$ and $\bar{V} = 2$, and we plot $\bar{h}(\bar{s},t)$ for $\bar{s} \in [0, 0.2]$ on Fig. 7.

The external flow thus breaks the left-right symmetry in two ways. First the average position of the cilium is not the vertical axis but a cilium curved in the direction of the flow. Second, the beating itself is no longer left-right symmetric: the cilium goes faster in the direction of the flow and comes back slower against the flow. The beating pattern looks like a two-phases beating with an effective stroke and a recovery stroke. The external flow may therefore be an important factor in the asymmetry of the beating.

Another important result, is that, because the beating propagates a base-to-tip deformation, the curved cilium exerts a finite average force in the fluid

in the direction of the flow. Thus, if an external flow breaks the left-right beating symmetry, the cilia create a force in its direction and can amplify this flow. This is the basis of the left-right spontaneous symmetry breaking that we discuss in the next section.

The external flow is not always the only source of symmetry breaking. If it were so, a *Paramecium* would always go in the same direction once it started moving. This is not the case, this organism is able to go backward when it bumps into an obstacle thanks to the release of calcium that reverses the beating.

The calculations of this section have been made with a velocity $\vec{V}$ uniform over the cilium length. This is not consistent with the presence of a cell wall where the cilium is anchored. Nevertheless, the main idea was to study how an external flow can break the beating symmetry in the simplest way. Similar calculations can be performed with a linearly varying velocity $\vec{V} = U\bar{z}$; they do not lead to any new physical effects.

4.2 Spontaneous breaking of the beating symmetry: array of aligned cilia

We now consider a regular array of cilia on a cell body, beating all in the same direction. Starting from a symmetrical beating, we show that the left-right symmetry is spontaneously broken within a certain range of the parameters controlling the beating due to the hydrodynamic couplings between cilia.

4.2.1 Equations of motion

For a cilium located in the xy plane at position $\vec{r}$, we call $\vec{V}[\vec{X}(s)]$ the velocity created by the other cilia at the point $\vec{X}(s)$ of arclength s. The equation of motion of the cilium is similar to that obtained previously with an external flow field and we write up to third order in h as

$$\xi_\perp \partial_t h = -\kappa \dddot{h} - a\dot{f} + \xi_\perp \vec{n}.\vec{V} + \mathcal{O}(h^3, \vec{t}.\vec{V}h) \tag{33}$$

where the projection of the local external velocity on the cilium normal is

$$\vec{n}.\vec{V} = V_x(1 - \dot{h}^2/2 - V_z\dot{h} + \mathcal{O}(h^4)) \tag{34}$$

The boundary conditions for the motion are the same as in the previous section.

The velocity $\vec{v}_j[\vec{X}_i(s_i)]$ created at arclength s_i of the cilium i by a cilium j is given by

$$\vec{v}_j[\vec{X}_i(s_i)] = \int_0^L ds_j \; \mathbf{G}[\vec{X}_i(s_i), \vec{X}_j(s_j)].\vec{f}_j[\vec{X}_j(s_j)]$$

where $\mathbf{G}$ is the second order hydrodynamic tensor given by Eq. 1 and $\vec{f}_j = \vec{f}_j^{beat}$ is the force per unit of length created by the beating of the cilium j. The total velocity at the arclength s_i of the cilium i is thus given by

$$\vec{V}[\vec{X}_i(s_i)] = \sum_{j \neq i} \vec{v}_j[\vec{X}_i(s_i)] = \vec{V}(\vec{r}_i, s_i, t) \tag{35}$$

As in section 2, we consider the limit $L \ll d$ and we only keep terms of the second order in s/r, r being the distance between cilia so that

$$\mathbf{G}.\vec{f} = \left([\mathbf{G}.\vec{f}_x].\vec{e}_x\right) \vec{e}_x + \mathcal{O}(s^3/r^3)$$

This means that only the velocity along the x axis created by the component f_x of $\vec{f}$ plays a role and that we can ignore the other component V_z of the velocity. Using the notations of Fig. 2, and noting that $z = s + \mathcal{O}(h^2)$, we obtain

$$V_x(\vec{r}_i, s_i, t) = \frac{3s_i}{2\pi\eta} \sum_{j \neq i} \frac{\cos^2\theta_{ij}}{|\vec{r}_i - \vec{r}_j|^3} \int_0^L ds_j f_{j_x}(s_j) s_j + \mathcal{O}(h^3, \frac{s^3}{r^3}) \tag{36}$$

As in the previous sections, we expand the velocity, the force and the cilium deformation in Fourier modes in time. For simplicity, we only consider here the first two Fourier components and do not look at the Fourier component h_2 that characterizes the asymmetry of the beating. The Fourier components of the velocity are related to the Fourier components of the force by

$$V_n(s_i) \simeq \frac{3s_i}{2\pi\eta} \sum_{j \neq i} \frac{\cos^2\theta_{ij}}{|\vec{r}_i - \vec{r}_j|^3} \int_0^L ds_j f_{j_n}(s_j) s_j$$

The Fourier components of the force $f_0 =< f_x >$ and f_1 are calculated

using the expression of f^{beat} and its average over one time period given by Eq. 52 in the small movements approximation:

$$\begin{aligned} f_0 &\simeq 2\omega(\xi_\perp - \xi_\parallel)\Im[2\dot{h}_0 h_1 \dot{h}_1^* - \dot{h}_1^* \int_0^s du \dot{h}_1(u)\dot{h}_0(u)] \\ f_1 &\simeq i\omega\xi_\perp h_1 \end{aligned} \tag{37}$$

where $\Im$ is the imaginary part of a complex number.

We assume that all cilia are identical, and that they all beat with the same pattern. The only difference in the beating patterns of cilia j and i is a possible phase difference that we call φ_{ij}. Defining

$$I_n = \int_0^L ds_i f_n(s_i) s_i$$

and dropping the index i, we write the Fourier components of the velocity as

$$\begin{aligned} V_0(s) &= \frac{3I_0 s}{2\pi\eta} \sum_{j\neq i} \frac{\cos^2\theta_{ij}}{|\vec{r}_i - \vec{r}_j|^3} = \frac{3\mathcal{K} I_0}{2\pi\eta d^3}\, s \\ V_1(s) &= \frac{3I_1 s}{2\pi\eta} \sum_{j\neq i} \frac{\cos^2\theta_{ij}}{|\vec{r}_i - \vec{r}_j|^3}\, e^{i\varphi_{ij}} = \frac{3\mathcal{K}[\{\varphi_{ij}\}] I_1}{2\pi\eta d^3}\, s \end{aligned} \tag{38}$$

The geometrical constant $\mathcal{K}$ is given by Eq. 7 for a square lattice of cilia spaced by d. The constant $\mathcal{K}[\{\varphi_{ij}\}]$ depends on the relative phases between the cilia. If the phases φ_{ij} are randomly distributed, then $\mathcal{K}[\{\varphi_{ij}\}] \simeq 0$ and $V_1 = 0$. There is no oscillating component of the velocity.

On the contrary, because we know that metachronism occurs in an array of beating cilia, we choose a constant phase difference φ between two consecutive cilia in the direction of the plane of beating : $\varphi_{i,j+1} - \varphi_{i,j} = \varphi$. This is the case for simplectic and antiplectic metachronal coordination. We only consider those cases (and not laeoplectic or dexioplectic metachronism) here. Experimentally, for *Opalina* (simplectic) and *Pleurobrachia* (antiplectic) that both have planar beatings, no metachronal wave in the transverse direction of the beating can be seen (25).

We stress that we do not impose the phase difference φ. The system is

free to adjust its phase. We then write $\mathcal{K}[\{\varphi_{ij}\}] = \mathcal{K}(\varphi)$ with

$$\mathcal{K}(\varphi) = \sum_{(k,l)\neq(0,0)} \frac{k^2 e^{ik\varphi}}{(k^2+l^2)^{5/2}} \tag{39}$$

Note that $\mathcal{K}(0) = \mathcal{K}$. The function $\mathcal{K}(\varphi)$ is plotted on Fig. 8 for a lattice of 10^6 cilia.

Note that for two particular values of φ that we denote by φ_s and φ_a this function vanishes, $\mathcal{K}(\varphi_s) = \mathcal{K}(\varphi_a) = 0$, as in the case where the relative phases of the cilia are randomly distributed. This corresponds to a constant flow with no oscillating component.

We now define the two dimensionless velocities U and $u(\varphi)$ by

$$\bar{U} = \frac{\xi_\perp L^3}{\kappa}\frac{3\mathcal{K} I_0 L}{2\pi\eta d^3} \qquad \bar{u}(\varphi) = \frac{\xi_\perp L^3}{\kappa}\frac{3\mathcal{K}(\varphi) I_1 L}{2\pi\eta d^3} \tag{40}$$

The equations of motions of the Fourier components $\bar{h}_0$ and $\bar{h}_1$ can then be written as

$$\begin{aligned} \dddot{\bar{h}}_0 - \bar{K}\ddot{\bar{h}}_0 &= \bar{U}\bar{s} \\ \dddot{\bar{h}}_1 + \bar{\chi}_1\ddot{\bar{h}}_1 + i\bar{\omega}\bar{h}_1 &= \bar{u}(\varphi)\bar{s} \end{aligned} \tag{41}$$

In writing Eq. 41, we only kept the term $\bar{U}\bar{s} = \mathcal{O}(h^3)$ that breaks the left-right symmetry and that lead to $h_0 \neq 0$, ignoring any other term that would not create a macroscopic motion.

4.2.2 Beating pattern and metachronal waves

We first study the equation of motion of the first Fourier mode in Eq. 41, which corresponds to the oscillatory motion of the cilium. The right hand side of this equation of motion does not vanish due to the existence of an oscillatory external flow due to the other cilia. Note however that we have not treated in details the hydrodynamic interactions for one cilium and that we have only taken them into account through the two local friction coefficients $\xi_\perp$ and $\xi_\parallel$. We are here more interested in the qualitative aspects of the coordination between cilia than in the accurate calculation of the flows created by each cilium.

The general solution of Eq. 41 can be written as $\bar{h}_1 = \bar{h}_1^h + \bar{h}_1^p$ with

$$\begin{aligned} \bar{h}_1^h(\bar{s}) &= A_1 e^{q_1 \bar{s}} + B_1 e^{-q_1 \bar{s}} + C_1 e^{q_2 \bar{s}} + D_1 e^{-q_2 \bar{s}} \\ \bar{h}_1^p(\bar{s}) &= \frac{\bar{u}(\varphi)}{i\bar{\omega}} \bar{s} \end{aligned} \tag{42}$$

It is convenient to rewrite the external velocity as $\bar{u}(\varphi) = i\bar{\omega}\mathbb{C}_1\gamma(\varphi)$ with

$$\gamma(\varphi) = \frac{3\mathcal{K}(\varphi)\xi_\perp L^3}{2\pi\eta d^3} \qquad \mathbb{C}_1 = \int_0^1 d\bar{s}\ \bar{h}_1(\bar{s})\bar{s} \tag{43}$$

The constant $\mathbb{C}_1$ can be determined self-consistently as it varies linearly with $\bar{h}_1$. We obtain

$$\bar{h}_1(\bar{s}) = \sum_i A_i (e^{q_i \bar{s}} + \beta(q_i, \varphi)\bar{s}) \tag{44}$$

with

$$\beta(q_i, \varphi) = \frac{\gamma(\varphi)}{1 - \gamma(\varphi)/3} \frac{q_i e^{q_i} - e^{q_i} + 1}{q_i^2} \tag{45}$$

The effect of the hydrodynamic interactions between cilia is embodied here in the coefficient $\gamma(\varphi)$. The variation of this coefficient with the phase difference φ is similar to that of $\mathcal{K}(\varphi)$. The limit where $\gamma(\varphi) = 0$, leads back to the previous situation were one cilium is beating alone; it may however correspond to the finite phase shifts between cilia $\varphi = \varphi_s$ or φ_a.

The four boundary conditions on $\bar{h}_1$ can as before be written in a matrix form and the oscillation threshold and the beating frequency can be determined as the zeros of a determinant insuring the consistency of this matrix equation. This leaves an unknown amplitude of the beating motion that could only be calculated by expanding the equation of motion to higher order. The beating pattern can then be written as

$$\bar{h}_1(\bar{s}) = \mathcal{A}_1[\mathcal{E}_\varphi(q_1, \bar{s}) + b_1\mathcal{E}_\varphi(-q_1, \bar{s}) + c_1\mathcal{E}_\varphi(q_2, \bar{s}) + d_1\mathcal{E}_\varphi(-q_2, \bar{s})]$$

with

$$\mathcal{E}_\varphi(q, \bar{s}) = e^{q\bar{s}} + \beta(q, \varphi)\bar{s}$$

The values of both the oscillation threshold Ω_c and the frequency $\bar{\omega}_c$ depend on the phase shift between cilia φ, through $\gamma(\varphi)$. We first discuss the variation of this bifurcation point with the constant $\gamma(\varphi)$ which is a more convenient variable. On Fig. 9, we plot Ω_c and the critical frequency f_c

against γ.

There is a local minimum of Ω_c for $\gamma^* \simeq -1.15$ and a local maximum for $\gamma \simeq 1$. The beating frequency f_c, is a decreasing function of γ.

We here need a selection criterion that determines the value of the phase shift between cilia. The simplest conjecture for the selection criterion is that the system chooses the local minimum of Ω_c corresponding to $\gamma^* \simeq -1.15$. This corresponds to a metachronal wave propagating in the assembly of cilia, as widely confirmed by experimental observations ((26, 27) for instance).

With this selection criterion, the oscillation threshold is $\Omega_c \simeq 6.538\ 10^{-9}$ and the critical frequency is $f_c \simeq 31Hz$. The hydrodynamical couplings between cilia decrease the oscillation threshold Ω_c and increase the critical frequency f_c. The coordination between cilia favors cilium beating by creating a metachronal wave corresponding to $\gamma < 0$.

The beating pattern is slightly changed as shown on Fig. 10 where we have plotted $2\Re[\bar{h}_1 e^{i\omega t}]$ at different time steps with the same amplitude $\mathcal{A}_1 = 1/70$.

The phase difference φ^* between two consecutive cilia corresponding to $\gamma^* \simeq -1.15$ depends on the values of the parameters. If we take $\eta = 4\eta_w$ and $d/L = 1$ so that our calculations remain consistent and in order to be close to what is observed experimentally, then $\mathcal{K}(\varphi^*) \simeq -0.07$ which yields $\varphi^* \simeq \pm 1.37 \simeq \pm 0.44\pi$. This value corresponds to a wavelength $\lambda = 4.6d \sim 5d$ for the metachronal waves or approximatively 6 cilia, which is the correct order of magnitude (the wave length is 7 cilia in (27)).

4.2.3 Global flow and left-right symmetry breaking

We now discuss the left-right symmetry breaking and the appearance of a global flow. We solve Eq. 41 for the zeroth Fourier component of the deformation, with the same boundary conditions as before, in the limit $\bar{K} \to 0$. We obtain

$$\bar{h}_0(\bar{s}) = \bar{U}\frac{\bar{s}^2}{6}(1 - \frac{\bar{s}}{2} + \frac{\bar{s}^3}{20}) \tag{46}$$

The cilium oscillates around a curved average position $\bar{h}_0 \neq 0$ if $\bar{U} \neq 0$, if there exists a global flow. We show below that this is possible within a certain range of parameters.

We define the two dimensionless functions

$$\begin{aligned} H_0(\bar{s}) = \frac{\bar{h}_0(\bar{s})}{\bar{U}} &= \frac{\bar{s}^2}{6}(1 - \frac{\bar{s}}{2} + \frac{\bar{s}^3}{20}) \\ H_1(\bar{s}) = \frac{\bar{h}_1(\bar{s})}{\mathcal{A}_1} &= \mathcal{E}_\varphi(q_1, \bar{s}) + b_1\mathcal{E}_\varphi(-q_1, \bar{s}) + c_1\mathcal{E}_\varphi(q_2, \bar{s}) + d_1\mathcal{E}_\varphi(-q_2, \bar{s}) \end{aligned}$$

The determination of the average velocity U requires the calculation of the integral of I_0 defined in Eq. 37; we obtain

$$I_0 = 2\mathbb{C}_\varphi {\mathcal{A}_1}^2 \bar{U}(\xi_\perp - \xi_\parallel)L^3\omega \tag{47}$$

with

$$\mathbb{C}_\varphi = \int_0^1 d\bar{s}\ \Im[2\dot{H}_0 H_1 \dot{H}_1^* - \dot{H}_1^* \int_0^{\bar{s}} d\bar{s}' \dot{H}_0 \dot{H}_1] \tag{48}$$

which can be numerically calculated knowing H_0 and H_1. $\mathbb{C}_\varphi$ depends on φ through H_1. Using the value of ϕ corresponding to metachronal waves, we obtain

$$\mathbb{C}_\varphi \simeq 34.5$$

A self-consistent equation is then be obtained for the average velocity $\bar{U}$

$$\bar{U} = \frac{3\mathcal{K}\mathbb{C}_\varphi(\xi_\perp - \xi_\parallel)L^3}{\pi\eta d^3} {\mathcal{A}_1}^2 \bar{\omega}\ \bar{U} \tag{49}$$

If $\mathbb{C}_\varphi < 0$ this equation has the only solution $U = 0$ and no global flow can exist, the left-right symmetry is not broken. If $\mathbb{C}_\varphi > 0$ this equation can have two extra non zero solutions $U \neq 0$ corresponding to a global flow along the x axis given by

$$< V(\bar{s}, t) >= V_0(\bar{s}) = U\bar{s}$$

and the left-right symmetry is then broken.

The condition for appearance of a global flow is

$$\frac{3\mathcal{K}\mathbb{C}_\varphi {\mathcal{A}_1}^2}{\pi} \frac{\xi_\perp - \xi_\parallel}{\eta} \frac{\xi_\perp L^4 \omega}{\kappa} \frac{L^3}{d^3} > 1 \tag{50}$$

As for the oscillation amplitude, our calculation only gives the threshold of appearance of the global flow. A determination of the actual value of the velocity would require an expansion of the equations of motion to higher

orders.

5 Discussion and concluding remarks

We have studied in this paper how hydrodynamic interactions between cilia contribute to the coordination of the beating motion in ciliated cells. Three major effects have been studied, the spontaneous alignment of an array of cilia, the breaking of the symmetry of the beating and the appearance of a macroscopic flow and the existence of metachronal waves. We have shown for all these problems that there exist a dynamic transition where symmetry is broken and where a coordination between the beating of neighboring cilia appears.

Our work is based on several simplifying approximations that we believe make the analysis tractable analytically but that should preserve the essential physical effects. We only studied hydrodynamic interactions between distant cilia that can be treated by introducing simple distribution of forces in the fluid to describe the motion of one cilium. This is rarely true experimentally but the hydrodynamic interactions between closer cilia are even stronger and strongly favor the transitions that we study. We have replaced the complex architecture of the axoneme by two microtubules sliding against one another under the action of dynein motors which are described by a two state model for molecular motors as done earlier by Camalet and Jülicher. This is a rather sketchy description but it allows a calculation of the internal forces that drive the cilium motion and it gives some physical insight. Future work will have to take into account the nine-fold symmetry of the axoneme and the influence of its central doublet. Finally, we have only considered small amplitude beating. This is sufficient to determine the oscillation threshold but it does not allow a quantitative comparison between the calculated beating and the experimental one that often occur far from any threshold. All our results are qualitatively consistent with the experimental observations and for example the beating frequency is close to both the experimental ones and to the ones obtained in numerical simulations (32).

The essential result of our work is the natural emergence of metachronal waves and of a macroscopic flow created by an array of cilia if the amplitude of beating is large enough. The criterion for appearance of the global uniform component of the flow given by Eq. 50 requires only very small amplitudes ($\mathcal{A}_1 \geq 5\ 10^{-4}$) which means that as long as the left-right symmetry

is broken, a macroscopic flow should appear. An essential ingredient for the macroscopic flow to appear is that the constant $\mathbb{C}_\varphi$ defined in Eq. 48 be positive so that the average force created by one cilium favors the flow and does not oppose it (which occurs if $\varphi = 0$).

As long as we allow a constant phase shift between neighboring cilia we observe metachronal coordination as a consequence of hydrodynamic interactions and of the internal beating mechanism of the cilium. A selection criterion is then needed for these waves. We have conjectured that the existing metachronal wave is the one that corresponds to the local minimum of the oscillation threshold. A more complete calculation that goes far beyond the scope of this work would have to consider the nucleation of the metachronal wave and to determine the fastest growing wave. One of the interesting predictions of our calculation is that the existence of metachronal waves leads to a flow which is far more stationary than if all the cilia were beating in synchrony. The oscillating component of the flow is proportional to the constant $\mathcal{K}(\varphi)$ (see Eq. 40) which has a much smaller value when metachronal waves exist ($\mathcal{K}(\varphi^*) \simeq -0.07$) than if all cilia are beating in synchrony ($\mathcal{K}(0) = \mathcal{K} \simeq 4.52$). Metachronism thus contributes to the creation of a very steady movement of swimming organisms that could for example make easier the detection of the organism environment.

Our most important conclusion is the idea that metachronism and the existence of macroscopic flow around ciliated organisms can exist as self-organized phenomena driven by hydrodynamic couplings. We must stress however that other mechanisms could be at the origin of these cooperative effects.

Aknowledgements : We thank A. Hilfinger, P. Dupuis-Williams, N. Spassky, M. Cosentino Lagomarsino, J. Prost and M. Bornens for useful discussions.

Appendix I: Average force created by a single beating cilium in a viscous fluid

The aim of this appendix is to calculate the force and momentum averaged over one time period created by a general periodic beating of a single cilium. We make two assumptions: the beating is planar and there is a stationary external flow. In section 4, the average flow is created by the neighboring

cilia.

We call ϕ the angle between the plane of beating and the direction of the external flow $\vec{V}$ that we take along the x axis. The cilium of length L is located at the origin and it is fixed at its basis. We denote by $h(s,t)$ the distance between a point at arclength s on the cilium and the z axis at time t and by $Z(s,t)$ the distance between a point at the arclength s on the cilium and the xy plane. The angle between the tangent vector $\vec{t}$ to the cilium and the z axis is denoted by $\psi(s,t)$ (see Fig. 11). The coordinates of the tangent vector are $\vec{t} = (\cos\phi \sin\psi, \sin\phi \sin\psi, \cos\psi)$. The angle ψ is related to the cilium deformation h by $\sin\psi = \partial_s h$

The point on the cilium at the arclength s is located at position $\vec{X} = (x,y,z)$, with:

$$\begin{aligned} x &= \cos\phi \int_0^s du \ \sin\psi(u,t) = h(s,t)\cos\phi \\ y &= \sin\phi \int_0^s du \ \sin\psi(u,t) = h(s,t)\sin\phi \\ z &= \int_0^s du \ \cos\psi(u,t) = Z(s,t) \end{aligned}$$

The velocity of this point is calculated by derivation with respect to time, $\vec{v} = \partial_t \vec{X}$.

The force per unit length exerted by the cilium on the fluid expressed in the Frenet basis $(\vec{t}, \vec{n}, \vec{b})$ is:

$$\vec{f} = (\xi_\parallel \vec{t}\,\vec{t} + \xi_\perp \vec{n}\,\vec{n} + \xi_\perp \vec{b}\,\vec{b})(\vec{v} - \vec{V}) \tag{51}$$

where $\xi_\parallel$ and $\xi_\perp$ are the two local friction coefficients for tangential and normal motion respectively. We decompose this force as a sum of two forces, $\vec{f}^{beat}$ depending on the local velocity and $\vec{f}^{flow}$ depending on the external flow velocity and calculate the average force over a beating period $< \vec{f} > = \frac{1}{T}\int_0^T dt \ \vec{f}(t)$.

The average beating force $< \vec{f}^{beat} >$ can be explicitly calculated

$$\begin{aligned}
< f_x^{beat} > &= (\xi_\perp - \xi_\parallel)\frac{\cos\phi}{2}\int_0^s du < \partial_t\psi(u)\cos\Delta(u,s) > \\
< f_y^{beat} > &= (\xi_\perp - \xi_\parallel)\frac{\sin\phi}{2}\int_0^s du < \partial_t\psi(u)\cos\Delta(u,s) > \\
< f_z^{beat} > &= -(\xi_\perp - \xi_\parallel)\frac{1}{2}\int_0^s du < \partial_t\psi(u)\sin\Delta(u,s) > \\
\Delta(u,s) &= 2\psi(s) - \psi(u)
\end{aligned} \tag{52}$$

This force is proportional to $(\xi_\perp - \xi_\parallel)$ as mentioned in section 2. The difference between the two local friction coefficients $\xi_\perp$ and $\xi_\parallel$ is at the basis of the flow generation by an assembly of beating cilia. Indeed, this is because the shape of the beating in the effective stroke is different from that in the recovery stroke that a force can be exerted in the fluid on average.

The average force due to the external flow is

$$\begin{aligned}
< f_x^{flow} > &= (\xi_\perp - \xi_\parallel)V\cos^2\phi < \sin^2\psi > -\xi_\perp V \\
< f_y^{flow} > &= (\xi_\perp - \xi_\parallel)V\cos\phi\sin\phi < \sin^2\psi > \\
< f_z^{flow} > &= (\xi_\perp - \xi_\parallel)V < \sin\psi\cos\psi >
\end{aligned}$$

It is important to note that $< f_x^{flow}(s) >< 0$: this force opposes the flow. The last term of f_x^{flow} is a static term, whereas the first positive term depends on the beating pattern and reduces the effects of this static term. In an assembly of cilia, the external velocity is due to the beatings of the other cilia which are themselves created by the forces on these cilia.

In section 2, we introduce a viscous coefficient α which characterizes the tendency for a cilium, beating in a plane at an angle ϕ with the flow, to align with the other cilia. A torque along the z axis due to the flow $M_z^{flow} = -\alpha U\sin\phi$ is exerted on this cilium. We now express α as a function of the cilium beating pattern. We call $m_z = -(\vec{X}\times\vec{f}).\vec{e}_z$ the torque along z exerted by the fluid on the cilium per unit of length (the minus sign is due to the fact that $\vec{f}$ is the force exerted by the cilium on the fluid). The local torque per unit length exerted by the fluid on the cilium is

$$m_z(s,t) = -\xi_\perp V h(s,t)\sin\phi = -\xi_\perp L\bar{h}(s,t)\bar{Z}(s,t)U\sin\phi$$

where we have used the dimensionless coordinates $\bar{s} = s/L$, $\bar{h} = h/L$. The

total momentum along z averaged over time, is obtained by integration

$$M_z = -\xi_\perp L^2 \int_0^1 d\bar{s} < \bar{h}(\bar{s},t)\bar{Z}(\bar{s},t) > \; U \sin\phi \tag{53}$$

This defines the friction coefficient α:

$$\alpha = \xi_\perp L^2 \int_0^1 d\bar{s} < \bar{h}(\bar{s},t)\bar{Z}(\bar{s},t) > \tag{54}$$

which can be calculated if the motion of the cilium is known.

Appendix II

In this appendix, we derive the equations satisfied by the Fourier components of the deformation h of a single beating cilium and we determine the threshold of spontaneous oscillations of the cilium.

Fourier mode expansion

Axoneme beating is periodic and can be studied by expansion in Fourier modes in time of all the physical parameters:

$$h(s,t) = \sum_{n=-\infty}^{\infty} h_n(s) e^{in\omega t}$$

The definition is similar for the other parameters. Starting from Eq. 17 and Eq. 14, we obtain the Fourier components:

$$\begin{aligned} f_n(s) &= -(K + in\omega\lambda)\Delta_n - \frac{1}{l}\int_0^l d\xi \; P_n(\xi)\partial_\xi W_1 \\ \Delta_{0n} &= \frac{1}{k + in\omega\gamma}\int_0^L ds f_n(s) \end{aligned} \tag{55}$$

In order to determine the non linear relationship between f and Δ, we follow the lines of (33) and write:

$$f_n = f_n^{(0)} + \sum_l f_{nl}^{(1)}\Delta_l + \sum_{lm} f_{nlm}^{(2)}\Delta_l\Delta_m + \mathcal{O}(\Delta^3)$$

The coefficients $f^{(k)}_{n,n_1,\ldots,n_k}$ can be calculated by first rewriting Eq. 16 as

$$P_n = R\delta_{n,0} - \frac{i\omega}{\nu(1+\Omega)} \sum_{lm} l\delta_{n,l+m}\Delta_l \partial_\xi P_m \tag{56}$$

where

$$R = \rho\frac{\omega_2(\xi)}{\omega_1+\omega_2} = \rho\frac{1+\Omega\sin^2(\pi\xi/l)}{1+\Omega}$$

is the static probability ($\omega = 0$), corresponding to a medium with not enough ATP to generate the beating. Inserting the ansatz

$$P_n = R\delta_{n,0} + \sum_l P^{(1)}_{nl}\Delta_l + \sum_{lm} P^{(2)}_{nlm}\Delta_l\Delta_m + \mathcal{O}(\Delta^3)$$

into Eq. 56, we obtain a recursion relation for the $P^{(k)}_{n,n_1,\ldots,n_k}$:

$$P^{(k)}_{n,n_1,\ldots,n_k} = -\frac{i\omega}{\nu(1+\Omega)} \sum_m n_k\delta_{n,n_k+m}\partial_\xi P^{(k-1)}_{m,n_1,\ldots,n_{k-1}}$$

that now allows us to calculate $f^{(k)}_{n,n_1,\ldots,n_k}$.

Our choice of a symmetric potential W_1 imposes that a change $\Delta \to -\Delta$ must change $f \to -f$. This symmetry imposes thus $f^{(2k)} = 0$. The only non-vanishing coefficient at linear order is $f^{(1)}_{nl} = \chi(\Omega, n\omega)\delta_{n,l}$ with

$$\chi(\Omega,\omega) = -K - \lambda i\omega + \frac{\pi^2\rho U}{2l^2}\frac{i\Omega\omega}{(1+\Omega)((1+\Omega)\nu + i\omega)} \tag{57}$$

The force and the sliding displacement are thus related by

$$f_n = \chi(\Omega, n\omega)\Delta_n + \mathcal{O}(|\Delta|^3) = \chi(\Omega, n\omega)(\Delta_{0n} + a\dot{h}_n + \mathcal{O}(|h|^3)) \tag{58}$$

This relationship 58 models the response of the molecular motors to the bending of the axoneme.

From Eq. 55 we obtain

$$\Delta_{0n} = \frac{\chi(\Omega, n\omega)a}{k + in\omega - \chi(\Omega, n\omega)L}h_n(L) + \mathcal{O}(|h|^3) \tag{59}$$

We solve the equation of motion of the cilium (Eq.18) for each order of the

Fourier expansion.

Equation of motion of the Fourier modes

We look for an approximate solution of the form

$$h(s,t) \simeq h_0(s) + h_1(s)e^{i\omega t} + h_2(s)e^{2i\omega t} + c.c.$$

At linear order, there is no coupling between the modes and using Eq.18, the equation of motion of the n^{th} Fourier component reads

$$\overset{....}{h}_n + \frac{\chi(\Omega, n\omega)a^2}{\kappa}\ddot{h}_n + i\frac{n\omega\xi_\perp}{\kappa}h_n = 0 \tag{60}$$

It is convenient to introduce the dimensionless variables:

$$\bar{s} = s/L \qquad \bar{\omega} = \frac{\xi_\perp L^4}{\kappa}\omega \qquad \bar{\chi}_n = \bar{\chi}(\Omega, n\bar{\omega}) = \frac{a^2L^2}{\kappa}\chi(\Omega, n\omega)$$

In dimensionless form, Eq. 57 can be written

$$\bar{\chi}(\Omega, \bar{\omega}) = -\bar{K} - \bar{\lambda}i\bar{\omega} + \frac{\pi^2}{2}\bar{\rho}\bar{U}\frac{i\ \Omega\bar{\omega}}{\bar{\nu} + i\bar{\omega}}$$

with

$$\bar{K} = \frac{a^2L^2}{\kappa}K \qquad \bar{\lambda} = \frac{a^2}{\xi_\perp L^2}\lambda \qquad \bar{\nu} = \frac{\xi_\perp L^4}{\kappa}\nu \qquad \bar{U} = \frac{a^2L^2}{\kappa l^3}U$$

We have anticipated here the fact that $\Omega \ll 1$.

Defining, $\bar{h} = h/L$, and denoting by a dot the derivation with respect to $\bar{s}$, we obtain the equation of motion Eq. 21 and the boundary conditions given by Eq. 22,23.

Beating motion

In the absence of external flow only the first Fourier component of h does not vanish and satisfies the equation of motion :

$$\overset{....}{\bar{h}}_1 + \bar{\chi}_1\ \ddot{\bar{h}}_1 + i\bar{\omega}\ \bar{h}_1 = 0 \tag{61}$$

where the relevant dimensionless parameters are

$$\bar{\chi}_1 = \bar{\chi}(\Omega, \bar{\omega}) \qquad \bar{\Gamma}_1 = \frac{\bar{\chi}_1^2}{\bar{k} - \bar{\chi}_1 + i\bar{\gamma}\bar{\omega}}$$

The boundary conditions are given by Eq. 22 and 23 for $n = 1$. The solution to this linear equation is a superposition of exponentials given by Eq. 24. The four boundary conditions on $\bar{h}_1$ can be written in a matrix form:

$$\mathbf{M}_1(\Omega, \bar{\omega}).\mathbf{A}_1 = 0 \tag{62}$$

where $\mathbf{A}_1$ is the vector made by the amplitudes of the exponentials in Eq. 24 and the matrix $\mathbf{M}_1$ is given by

$$\mathbf{M}_1(\Omega, \bar{\omega}) = \begin{bmatrix} 1 & 1 & 1 & 1 \\ q_1 & -q_1 & q_2 & -q_2 \\ \mathcal{F}(q_1) & \mathcal{F}(-q_1) & \mathcal{F}(q_2) & \mathcal{F}(-q_2) \\ q_1^2 e^{q_1} & q_1^2 e^{-q_1} & q_2^2 e^{q_2} & q_2^2 e^{-q_2} \end{bmatrix}$$

with

$$\mathcal{F}(q) = e^q(q^3 + \bar{\chi}_1 q + \bar{\Gamma}_1)$$

The system 62 has non trivial solutions only if

$$\det \mathbf{M}_1(\Omega, \bar{\omega}) = 0 \tag{63}$$

Since Eq. 63 is a complex equation, it determines both the oscillation threshold Ω_c and the dimensionless beating frequency $\bar{\omega}_c$.

References

1. Alberts, B., D. Bray, J. Lewis, M. Raff, K. Roberts, and J. Watson. 1994. Molecular Biology of the Cell. Garland, New York.

2. Anderson, R. 1972. The three-dimensional structure of the basal body from rhesus monkey oviduct. J. Cell. Biol. 54:246–265.

3. Sleigh, M. 1962. The Biology of Cilia and Flagella. Pergamon Press, Oxford.

4. Hagiwara, H., N. Ohwada, and K. Takata. 2004. Cell biology of normal and abnormal ciliogenesis in the ciliated epithelium. Int. Rev. Cytol. 234:101–141.

5. Porter, M. and W. Sale. 2000. The 9 + 2 axoneme anchors multiple inner arm dyneins and a network of kinases and phosphatases that control motility. J. Cell. Biol. 151:F37–F42.

6. Wargo, M. and E. Smith. 2003. Asymmetry of the central apparatus defines the location of active microtubule sliding in Chlamydomonas flagella. Proc. Natl. Acad. Sci. USA. 100:137–142.

7. Camalet, S. 2001. Oscillations critiques de systèmes biologiques. Ph.D. thesis, Université Paris VI, Paris.

8. Camalet, S. and F. Jülicher. 2000. Generic aspects of axonemal beating. New J. Phys. 2:24.1–24.23.

9. Naitoh, Y. and H. Kaneko. 1972. Reactivated triton extracted models of Paramecium: modification of ciliary movement by calcium ions. Science. 176:523–524.

10. Naitoh, Y. and H. Kaneko. 1973. Control of ciliary activities by adenosine triphosphate and divalent cations in Triton-extrated models of Paramecium caudatum. J. Exp. Biol. 58:657–676.

11. Gibbons, I. 1961. The relationship between the fine structure and direction of beat in gill cilia of a lamellibranch mollusc. J. Biophys. Biochem. Cytol. 11:179–205.

12. Sorokin, S. 1968. Reconstructions of centriole formation and ciliogenesis in mammalian lungs. J. Cell. Sci. 3:207–234.

13. Boisvieux-Ulrich, E., M. Laine, and D. Sandoz. 1985. The orientation of ciliary basal bodies in quail oviduct is related to the ciliary beating cycle commencement. Biol. Cell. 55:147–150.

14. Afzelius, B. 1979. The immotile-cilia syndrome and other ciliary diseases. Int. Rev. Exp. Path. 19:1–43.

15. Liron, N. and S. Mochon. 1976. The discrete cilia approach to propulsion of ciliated micro-organisms. J. Fluid. Mech. 75:593–607.

16. Blake, J. 1971. A note on the image system for a stokeslet in a no slip boundary. Proc. Camb. Phil. Soc. 70:303–310.

17. Beisson, J. and M. Jerka-Dziadosz. 1999. Polarities of the centriolar structure: morphogenetic consequences. Biol. Cell. 91:367–378.

18. Gradshteyn, I. and I. Ryzhik. 1980. Table of integrals, series and products. Academic Press, Orlando.

19. Borwein, J. M. and P. B. Borwein. 1987. Pi and the AGM: A Study in Analytic Number Theory and Computational Complexity. Wiley, New York. 291. http://mathworld.wolfram.com/DoubleSeries.html.

20. Hilfinger, A. 2005. Dynamics of Cilia and Flagella. Ph.D. thesis, Technische Universität, Dresden.

21. Vernon, G. and D. Woolley. 2004. Basal sliding and the mechanics of oscillation in a mammalian sperm flagellum. Biophys. J. 87:3934–3944.

22. Prost, J., J.-F. Chauwin, L. Peliti, and A. Adjari. 1994. Asymmetric pumping of particles. Phys. Rev. Lett. 72:2652–2656.

23. Jülicher, F. and J. Prost. 1995. Cooperative molecular motors. Phys. Rev. Lett. 75:2618–2622.

24. Ishijima, S. and Y. Hiramoto. 1994. Flexural rigidity of echinoderm sperm flagella. Cell Struct. Funct. 19:349–362.

25. Murase, M. 1992. The dynamics of cellular motility. Wiley, Chichester.

26. Horstmann, E. 1959. Epithelium vibrans (Flimmerepithel). Movie, IWF, Göttingen. http://mkat.iwf.de.

27. Machemer, H. 1972. Ciliary activity and the origin of metachrony in Paramecium: effects of increased viscosity. J. Exp. Biol. 57:239–259.

28. Gueron, S. and K. Levit-Gurevich. 1998. Computation of the internal forces in cilia: application to ciliary motion, the effects of viscosity, and cilia interactions. Biophys. J. 74:1658–1676.

29. Sugrue, P., M. Hirons, J. Adam, and H. M.E. 1988. Flagellar wave reversal in the kinetoplastid flagellate Crithidia oncopelti. Biol. Cell. 63:127–131.

30. Hayashi, M., T. Yagi, Y. K., and R. Kamiya. 1998. Real-time observation of Ca^{2+}-induced basal body reorientation in Chlamydomonas. Cell. Motil. Cytoskeleton. 41:49–56.

31. Cosentino Lagomarsino, M., B. Bassetti, and P. Jona. 2002. Rowers coupled hydrodynamically. Modeling possible mechanisms for the cooperation of cilia. Eur. Phys. J. B. 26:81–88.

32. Gueron, S., K. Levit-Gurevich, N. Liron, and J. Blum. 1997. Cilia internal mechanism and metachronal coordination as the result of hydrodynamical coupling. Proc. Natl. Acad. Sci. USA. 94:6001–6006.

33. Jülicher, F. and J. Prost. 1997. Spontaneous oscillations of collective molecular motors. Phys. Rev. Lett. 78:4512–4516.

Tables

Table 1.

Decrease of the beating frequency with increasing external viscosity as observed in experiments (27). Comparison with the simulations done in (28) for one single cilium.

External viscosity	Critical frequency f_c	Simulations
η_w	$28Hz$	$29Hz$
$2\eta_w$	$19Hz$	$17Hz$
$3\eta_w$	$14Hz$	$12Hz$

Table 1: Viscosity and beating frequency

Figure Legends

Figure 1.

a) Beating pattern of a single cilium showing the Effective Stroke (ES), where the fluid is efficiently propelled, and the slower Recovery Stroke (RS), where the cilium comes back close to the surface to minimize the viscous effects. b) Effective force in the fluid $\vec{f}$ applied at a height h above the cell membrane, to mimic the cilium beating.

Figure 2.

Square lattice of cilia with a distance d between two neighboring cilia. Cilium j exerts on the fluid a force f in the direction ϕ_j; $\theta_{ji} = (\vec{e_x}, \vec{e_{ji}})$ where $\vec{e_{ji}}$ is the unit vector from cilium j to cilium i.

Figure 3.

Two filaments (full curves) $\vec{X}$ and $\vec{X}'$ at constant separation a are rigidly connected at the bottom end where $s = 0$. Internal forces $f(s)$ are exerted in opposite directions, tangential to the filaments. The displacement Δ at the tip is indicated.

Figure 4.

Approximate cilium deformation $\bar{h}(\bar{s}, t)$ at different times steps (corresponding to different colors) during a beating period. The beating is symmetrical with respect to the vertical axis. Deformations are propagating from base to tip. With $\mathcal{A}_1 = 1/70$ the maximum deformation is $\bar{h}_{max} \simeq 0.14$.

Figure 5.

Effect of an external flow $\vec{V}$ on the beating of a single cilium. *a*) Symmetrical beating. *b*) broken symmetry due to the external flow.

Figure 6.

a) Average position of a cilium which is curved in the direction of the flow, $\bar{h}_0(\bar{s}) =< \bar{h}(\bar{s}, t) >$. *b*) Second Fourier component of the deforma-

tion $2\Re[\bar{h}_2(\bar{s})e^{2i\omega t}]$ at different times during a beating period. The scale is dilated: $|\bar{h}_2| \ll 0.1$ with the parameters $\bar{\xi} = 1$, $\mathcal{A}_1 = 1/70$ and $\bar{V} = 1$.

Figure 7.

Beating pattern at the basis of the cilium ($\bar{s} \in [0, 0.2]$) with the parameters $\bar{\xi} = 1$, $\mathcal{A}_1 = 1/5$ and $\bar{V} = 2$: the cilium beats faster in the direction of the flow and slower in the opposite direction around a curved average position.

Figure 8.

$\mathcal{K}(\varphi)$ over one period ($\varphi \in [0, 2\pi]$). Some remarkable values: $\mathcal{K}(0) = \mathcal{K}_{max} \simeq 4.52$; $\mathcal{K}(\pi) = \mathcal{K}_{min} \simeq -2.32$; $\mathcal{K}(\varphi_s) = \mathcal{K}(\varphi_a) = 0$ with $\varphi_s \simeq 1.34$ and $\varphi_a \simeq 4.94$.

Figure 9.

Oscillation threshold Ω_c and critical frequency f_c as functions of γ for $\gamma \in [-3, 2]$. Ω_c has a local minimum that corresponds to the existence of metachronal waves.

Figure 10.

Beating pattern of a cilium in an array in the presence of a metachronal wave. The pattern is different from that of an isolated cilium mostly around the basis. The first Fourier component $2\Re[\bar{h}_1 e^{i\omega t}]$ at various time steps during a period is plotted. The parameters are $\mathcal{A}_1 = 1/70$; the maximum deformation is $\bar{h}_{max} \simeq 0.15$.

Figure 11.

Sketch of a beating cilium in a plane at an angle ϕ with the direction of the external flow V.

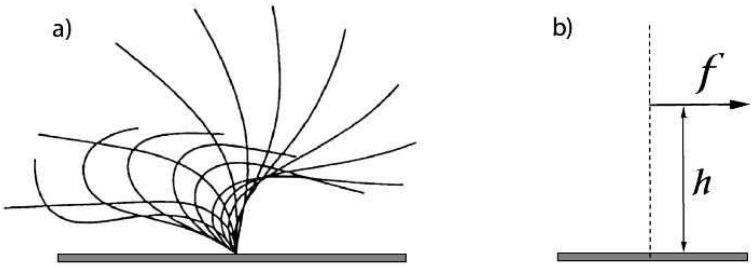

Figure 1: ...

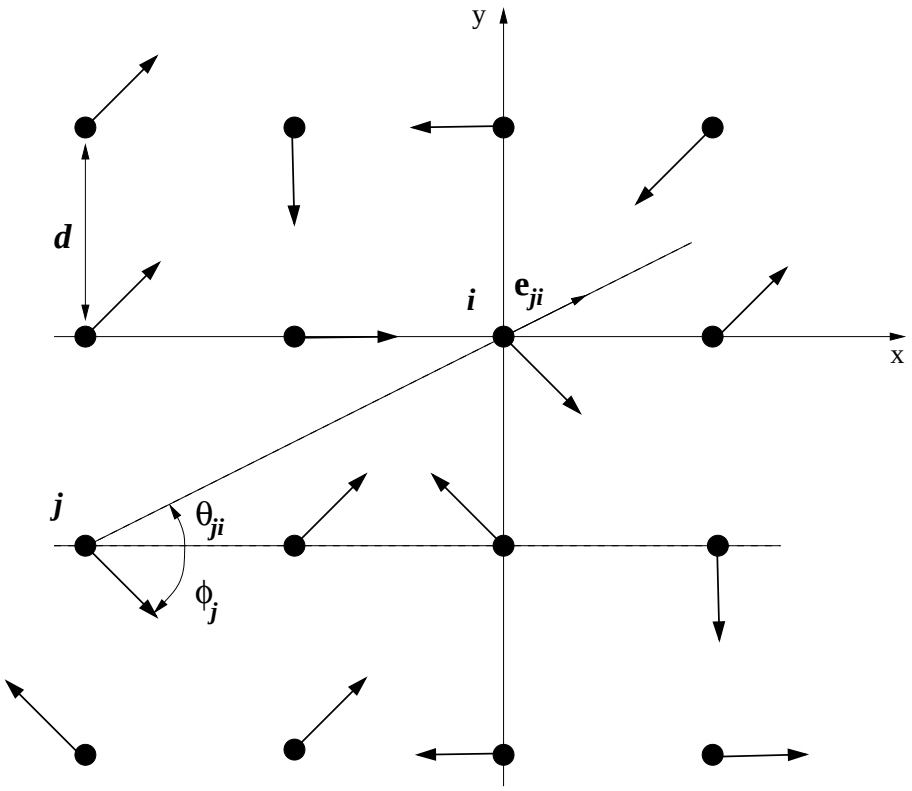

Figure 2: ...

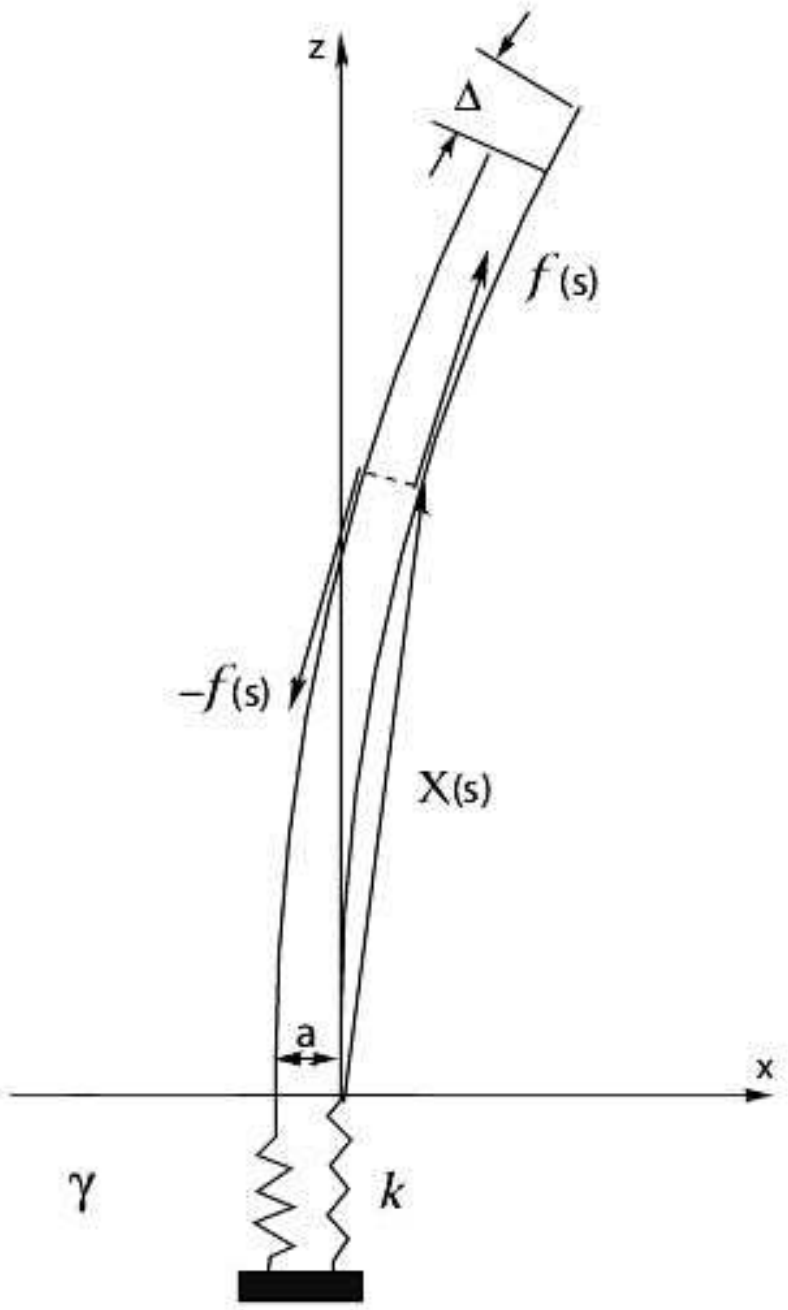

Figure 3: ...

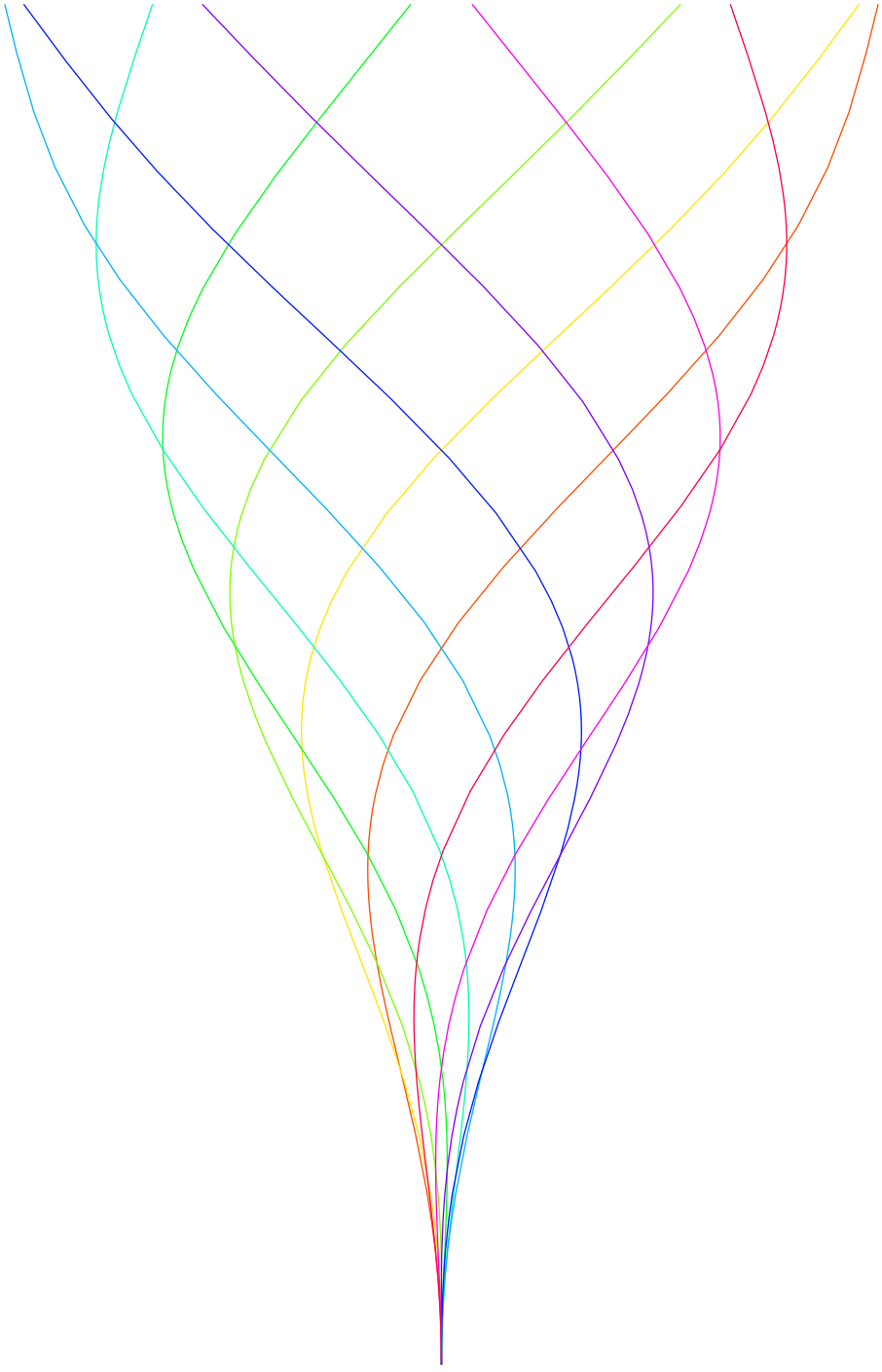

Figure 4: ...

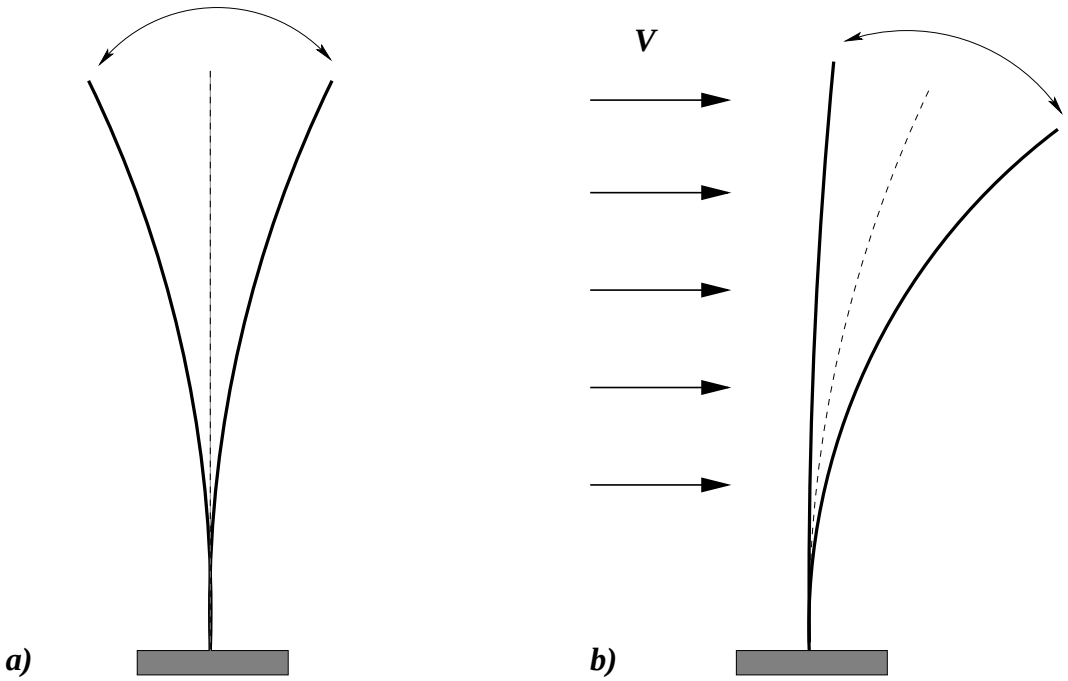

Figure 5: ...

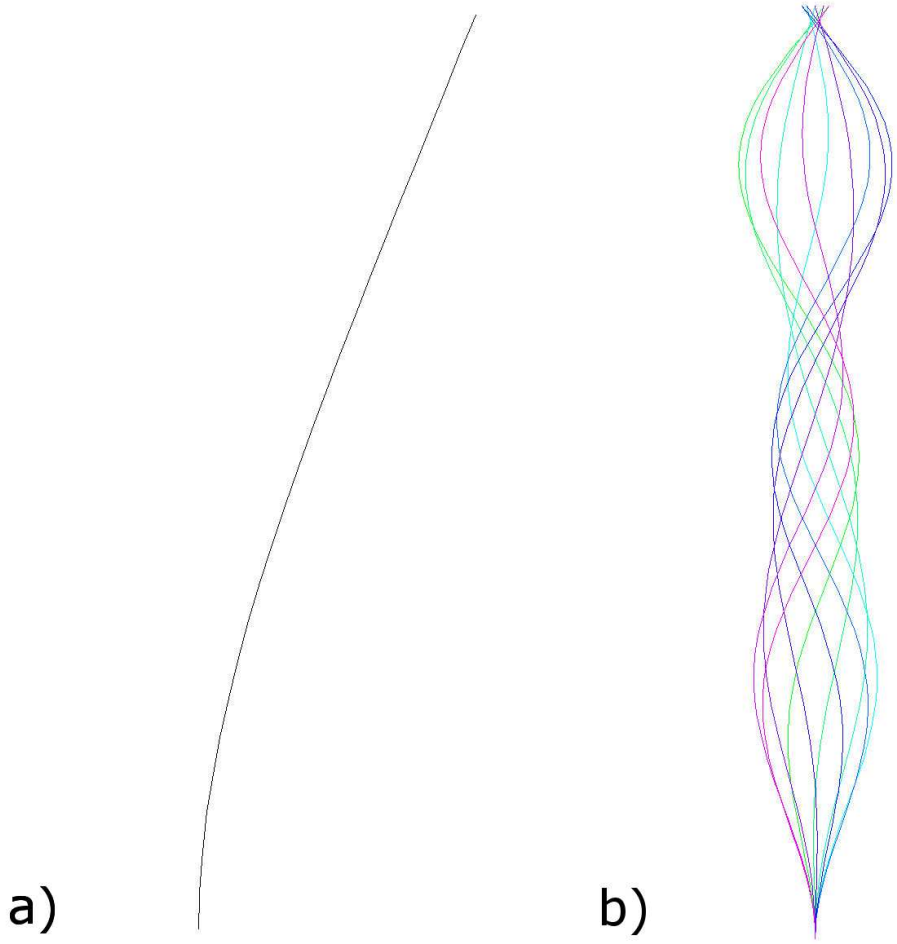

Figure 6: ...

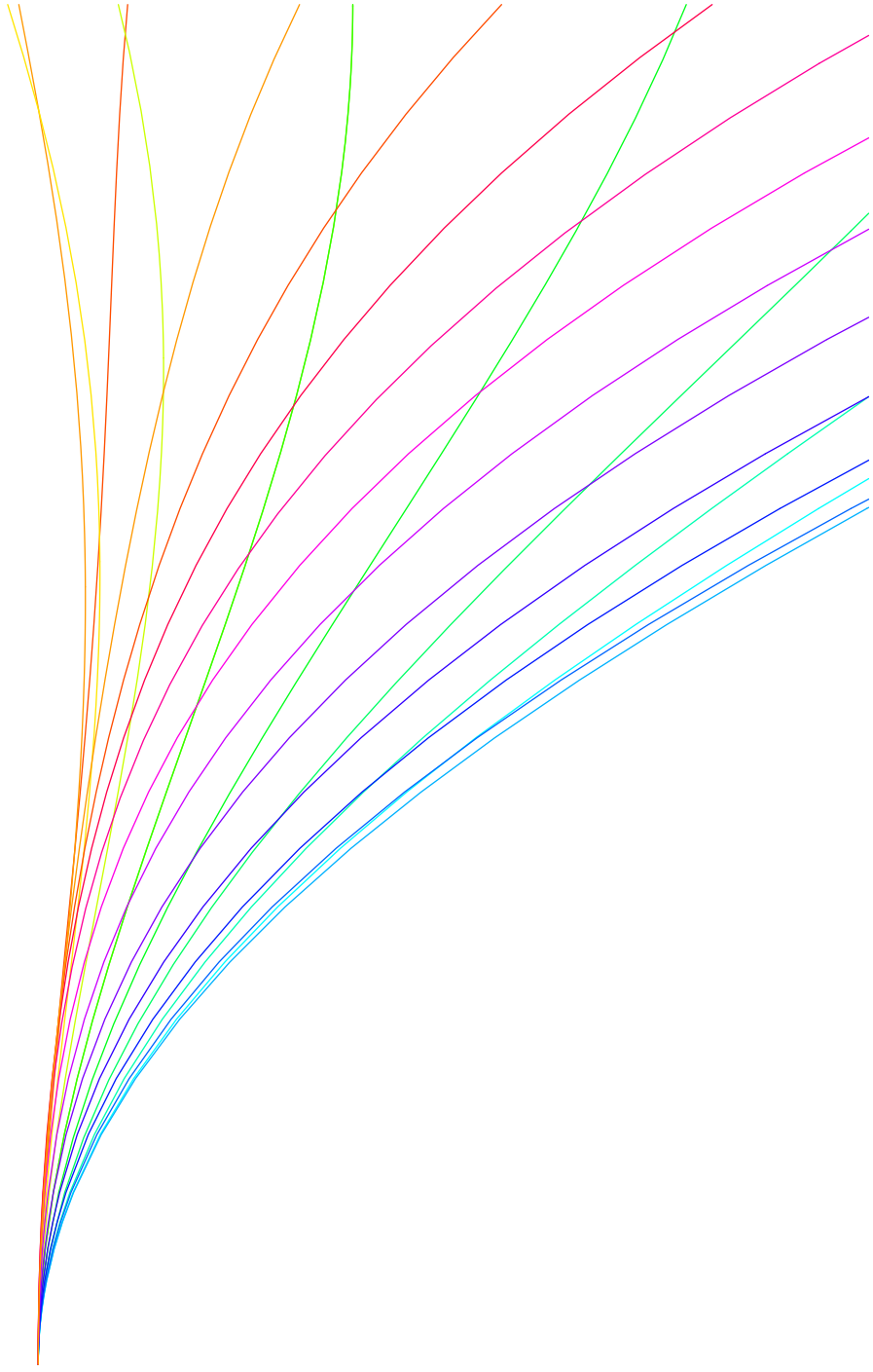

Figure 7: ...

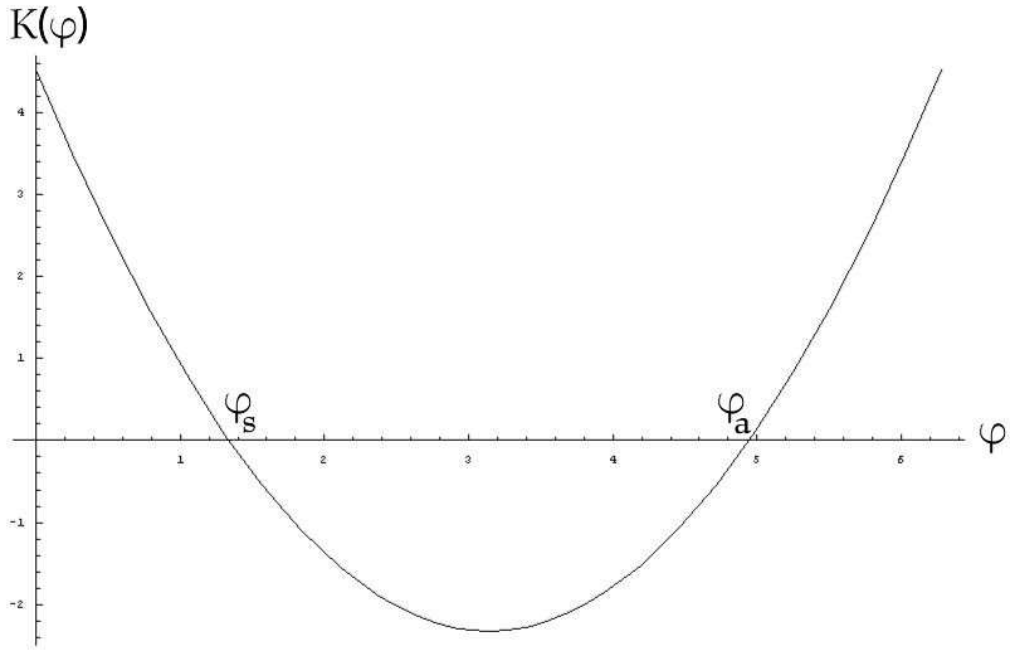

Figure 8: ...

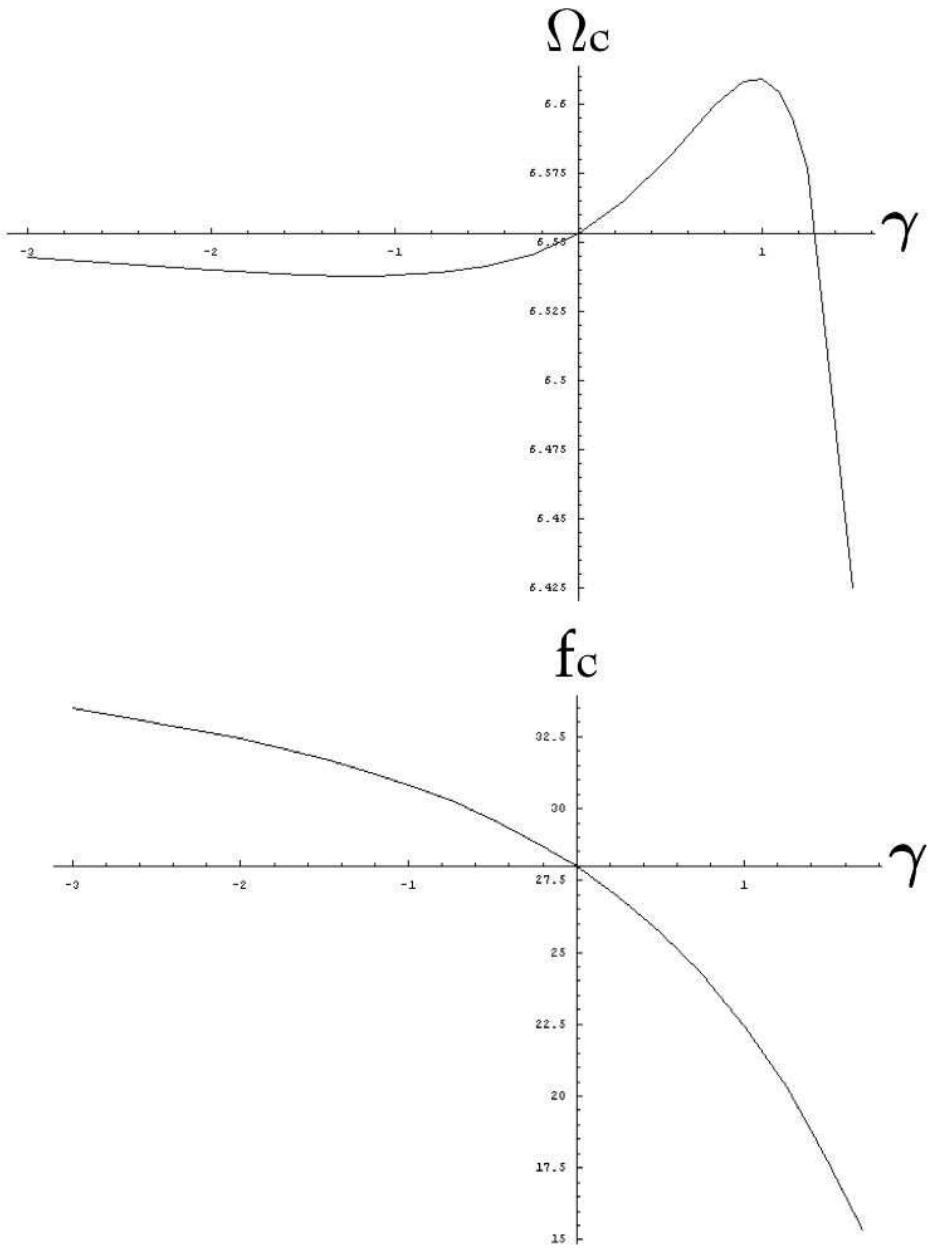

Figure 9: ...

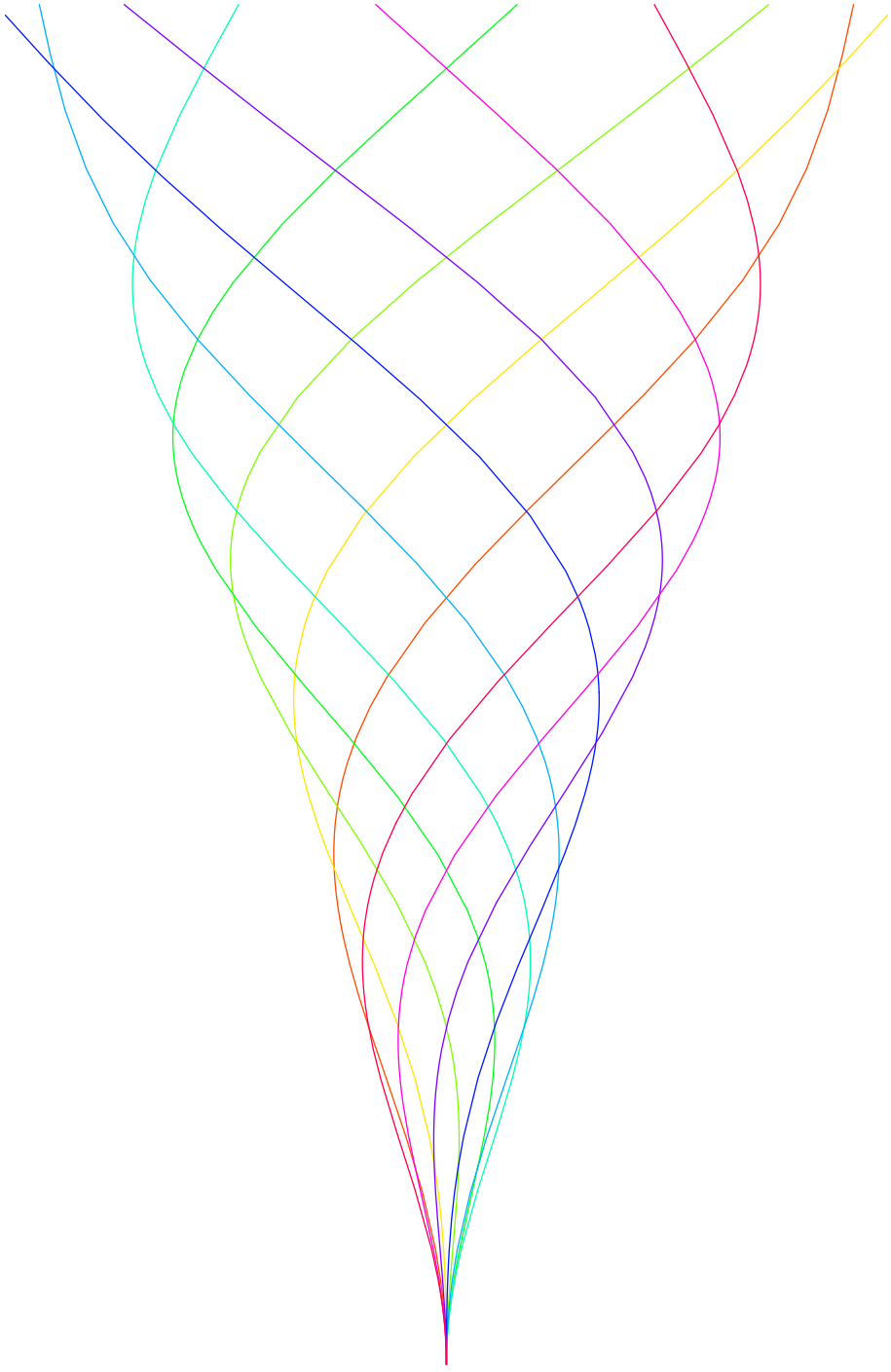

Figure 10: ...

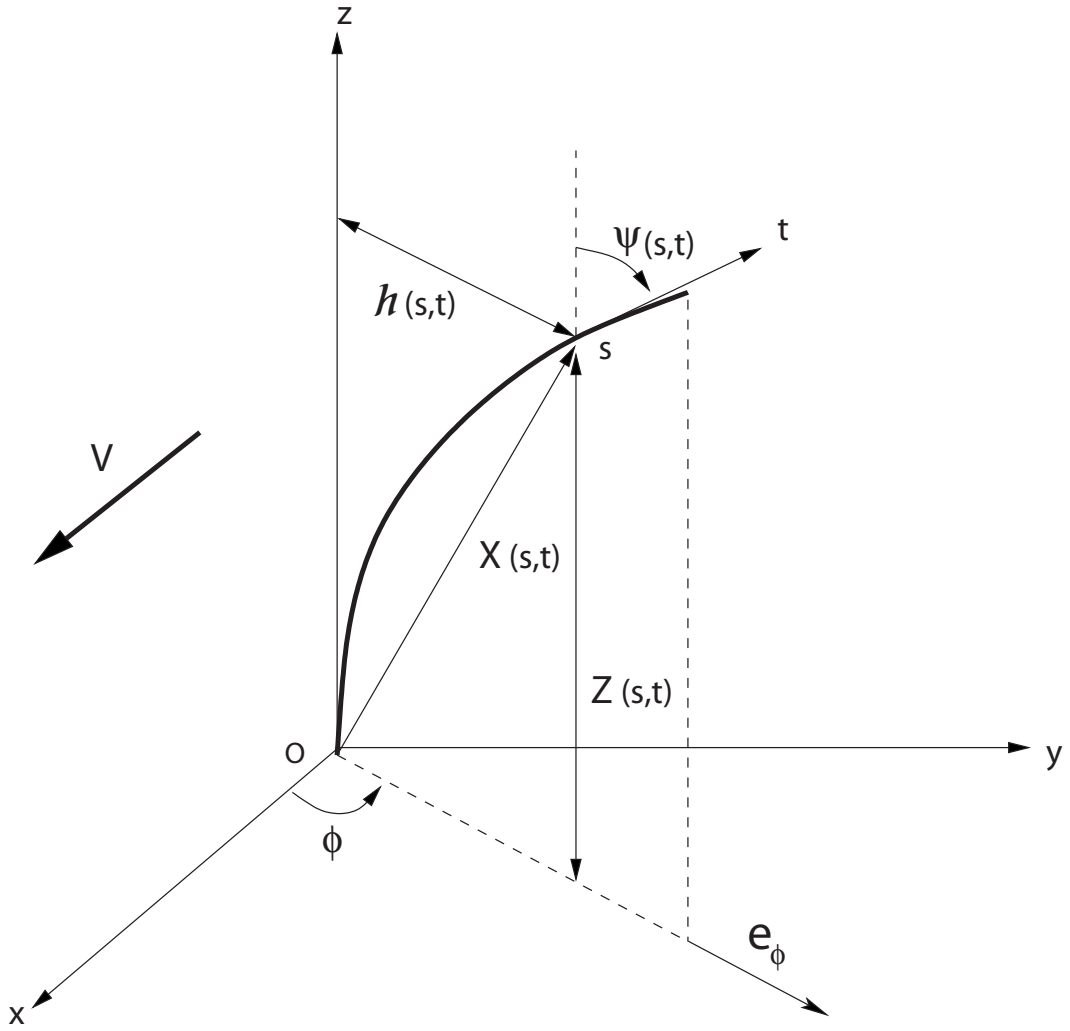

Figure 11: ...